CALIBRATION OF COSMIC-RAY SOIL NEUTRON SENSORS (CRNS) IN DIFFERENT LAND USE-LAND COVERS IN LOWER BRAZOS RIVER BASIN: A MODELING APPROACH

A Thesis

by

SIDDHARTH SINGH

Submitted to the Office of Graduate and Professional Studies of
Texas A&M University
in partial fulfillment of the requirements for the degree of

MASTER OF SCIENCE

Chair of Committee,	Binayak Mohanty
Committee Members,	Gretchen Miller
	Haly Neely
Interdisciplinary Faculty Chair,	John Giardino

August 2019

Major Subject: Water Management and Hydrological Science

ABSTRACT

The cosmic-ray neutron sensors (CRNS) are a proximal sensor that can be used to estimate spatially averaged soil moisture at hectometer scale. The sensor measures the number of thermalized neutrons created by the collision between cosmic rays and atmosphere that interact with hydrogen atoms present in the environment and can be used to estimate soil moisture. However, extensive in-situ soil moisture measurements are needed to separate the signal of soil moisture from all other hydrogen pools such as aboveground biomass and atmospheric water content to calibrate the sensor. The objective of this study is to introduce a new technique of calibrating the sensor by evaluating water budget closures using CRNS and a calibrated sub-surface model Hydrus with minimal ground measurements. We installed CRNS at three sites in the Brazos river basin representing different land covers and management practices: i) traditional agriculture, ii) native prairie, and iii) managed prairie. The model was parameterized by inverting profile soil moisture information from just three locations in each land cover using the Shuffled Complex Evolution Algorithm in Hydrus-1D. The hydraulic parameters for the entire field were estimated by interpolating between the three locations to populate a Hydrus 2D model domain which was used to simulate the soil moisture distribution in the field. The CRNS was calibrated against the area average of modeled soil moisture distribution in the field. The calibrated dataset was able to capture the soil water budget at all the three sites with a water budget closure error of 0.01 m^3m^{-3}-0.07 m^3m^{-3}. The first part of validation was done by evaluating the calibrated output against intensively measured gravimetric soil moisture. We achieved acceptable values of RMSE (0.03m^3m^{-3}- 0.06 m^3m^{-3}).For second part of validation we compare the evapotranspiration (ET) derived from Landsat

thermal sensors and calibrated CRNS output. The ET from Landsat 8 was derived using METRIC algorithm which solves energy balance equation to provide the estimates. The values are calibrated against the reference ET acquired using Penman-Monteith equation. ET from CRNS is calculated using piecewise linear regression model. CRNS performed better than the Landsat-ET and has higher temporal resolution. The method reduces the labor in the regions where conducting field campaigns is difficult. Additionally, CRNS presents itself as a viable alternative to in-situ electromagnetic sensors in the clayey soil where the performance of these sensors is poor due to signal distortion.

DEDICATION

To my dear parents, advisor and friends, for their patience and encouragement

ACKNOWLEDGEMENTS

I would like to thank my committee chair, Professor Binayak Mohanty, and members, Professor Gretchen Miller, and Professor Haly Neely, for their guidance and support throughout the course of this research.

I would also like to thank my mentor Nandita Gaur, who gave me valuable insight and taught me necessary tools which helped in completion of this project.

I am grateful to my friends and colleagues from the Vadose Zone Research Group and the department faculty for making my time at Texas A&M University a great experience.

Special regards go to all the Principal Investigators and students involved in Texas Water Observatory, who provided me valuable dataset to carry out this project.

Finally, thanks to my mother and father for their encouragement and patience.

CONTRIBUTORS AND FUNDING SOURCES

Contributors

This work was supported by a thesis committee consisting of Professor Binayak P. Mohanty of the Department of Biological and Agricultural Engineering, Professor Gretchen Miller of the Department of Civil Engineering and Professor Haly Neely of the Department of Soil and Crop Sciences.

The data analyzed was provided by Texas Water Observatory with Professor Binayak P. Mohanty as the Principal Investigator.

All the work conducted for the thesis was completed by the student independently.

Funding Sources

Graduate study was supported by a fellowship from School of Geosciences and Texas Water Observatory.

NOMENCLATURE

CRNS	Cosmic Ray Neutron Sensors
ET	Evapotranspiration
SWI	Soil wetness index
MISDc	Modello Idrologico SemiDistribuito in continuo
ENVISAT	Environmental satellite
SMOS	Soil Moisture and Ocean Salinity
SMAP	Soil Moisture Active Passive
TDR	Time domain reflectometry
CS	Capacitance sensor
SGP'99	1999 Southern Great Plains Experiment
SMEX02	Soil Moisture Experiments in 2002
CAROLS	Cooperative Airborne Radiometer for Ocean and Land Studies
TWO	Texas Water Observatory
SN	Soil node
TFPR	TFPR Farm Prairie
CS650	Campbell Scientific 650
NED	National Elevation Dataset
EC	Electrical conductance
SCE-UA	Shuffled Complex Evolution Algorithm
NDVI	Normalized Difference Vegetation Index
WSS	Web Soil Survey

RMSE	Root Mean Square Error
C/S	Cross Sectional
EM-38	Electromagnetic Induction Sensor
ETDI	Evapotranspiration Deficit Index
SPEI	Standardized Precipitation Evapotranspiration Index
TIR	Thermal Infrared
VNIR	Visible Near-Infrared
METRIC	Mapping ET at high Resolution with Internalized Calibration
METRIC-ET	Evapotranspiration Derived from Landsat using METRIC Algorithm
TM	Thematic Mapper
DEM	Digital Elevation Model
LAI	Leaf Area Index
LE	Latent Energy
G	Ground Heat Flux
H	Sensible Heat Flux
LAI	Leaf Area Index
SEBAL	Surface Energy Balance
CIMEC	Calibration using Inverse Modeling at Extreme Conditions
CRNS-ET	Evapotranspiration Derived from CRNS

TABLE OF CONTENTS

LIST OF FIGURES

Page

LIST OF TABLES

CHAPTER I

INTRODUCTION

1.1 Importance of Soil Moisture at Different Scales

Soil moisture is a crucial variable for closing the water budget from local to global scales. It is critical for diverse applications ranging from climate-change studies, disaster mitigation to irrigation scheduling for better farming practices (Henderson-Sellers 1996; Dai et al., 2004; Campbell et al., 1982).At continental scales, hydrologic models use estimates of soil moisture to partition total water storage into individual components (Hoekstra et al., 2012; Rodell et al., 2009). Assessment of large-scale soil moisture deficit is the backbone of various drought indices (Narsimhan et al., 2005; Alley 1984). Past studies have suggested a positive correlation between negative soil moisture anomalies and severity of extreme events such as heat waves (Lorenz et al., 2010; Stefanon et al., 2014). Global soil moisture datasets have been used to calibrate rainfall-runoff models (Soorooshian et al., 1993; Hong et al., 2007). At the catchment scale, characterization of soil moisture distribution is essential for various hydrological applications (Matgenet al., 2012). For example, Soil wetness index (SWI) was developed and assimilated in runoff model MISDc ("Modello Idrologico SemiDistribuito in continuo") and validated against the model's flood prediction capabilities (Brocca et al., 2010). Additionally, soil erosion models make use of soil moisture to quantify the soil degradation in a river basin (Jetten et al., 1999).

Catchment scale soil moisture is often validated using in-situ point scale dataset (Malbéteauet al., 2016; Montzka et al., 2012). In addition to remotely sensed soil moisture,

point scale soil moisture is used in the calibration and validation of several land surface models (Crow et al., 2003; Koster et al., 2009).It is used to study the impact of soil texture, topography, and vegetation to spatio-temporal variability in soil moisture distribution (Mohanty et al., 2000a,b; Mohanty and Skaggs, 2001; Joshi et al. 2010). Point scale soil moisture can be used to determine field scale moisture.

Point or catchment scale data are used to determine field scale soil moisture estimates (Martínez-Fernández et al., 2005; Wang et al., 2015; Merlin et al., 2008).Strong correlation is observed between field scale and spatially dominant hydrological processes (Western et al., 2004; Kirkby et al., 1996). Accurate estimation of field scale soil moisture also has large economic implications in precision agriculture (Cai et al., 2003; Münier et al., 2004). Starr (2005), observed higher yields by maintaining temporally stable soil moisture conditions by comparing various irrigation practices. Muñoz-Carpena et al., (2015) observed a reduction of 50% in water usage after switching to soil moisture-based irrigation scheduling.

1.2 Motivation: Measuring Soil Moisture at Multiple Scales

Remote sensing of soil moisture uses microwave frequency bands and contrasting dielectric properties of soil and water. Coarse-scale data, obtained from satellites such as Environmental Satellite(ENVISAT) , Soil Moisture and Ocean Salinity (SMOS), and Soil Moisture Active Passive (SMAP) can provide soil moisture estimates at high temporal resolution (2-5 days) but low spatial resolution (25-50km) (Mohanty et al., 2017), that may perform reasonably for large-scale hydrological studies but cannot capture the heterogeneity at a field scale.

Historically, in-situ measurements have adequately captured small-scale spatial and temporal variability in soil moisture distribution (Mohanty et al., 2000a,b; Jacobs et al., 2004). At point support, gravimetric soil moisture determined using oven drying method is still the most accurate (and only direct method) used to calibrate and compare soil moisture obtained from indirect methods(Huisman et al., 2001; Leib et al., 2003). The indirect methods use soil dielectric or thermal properties combined with empirical equations to determine soil water content. Mittelbach et al.,(2012), studied indirect methods such as time domain reflectometry (TDR), capacitance (CS) and frequency domain reflectometry-based probes and found high errors in soils with high clay contents. Datta et al., (2018), found overestimation of field capacity and wilting point by TDR and CS probes in soils with high clay contents.

At a field scale, soil moisture observations from airborne microwave sensors are available through intensive field campaigns such as the1999 Southern Great Plains Experiment (SGP'99) in Oklahoma, Soil Moisture Experiments in 2002(SMEX02) in Iowa, and Cooperative Airborne Radiometer for Ocean and Land Studies in Valencia, Spain(CAROLS) (Njoku et al., 2002 ; McCabe et al.,2005; Albergel et al.,2011). However, conducting such campaigns is expensive and therefore cannot be used on an operational scale.

Thus, to get better estimates of soil moisture at the field scale, top-down (downscaling) or bottom-up scaling (upscaling) approaches are employed using satellite or in-situ datasets. Downscaling of satellite data can be done by fusing active and passive satellite observation (Njoku et al., 2002; Narayan et al., 2006; Das et al., 2006). Downscaling can be performed using land surface models. Deterministic or stochastic models are used to transfer parameters across scales by manipulating input variables and calibrating the models comparing the outputs and

observations (Wu et al., 2006, Shin et al., 2013). Upscaling can be performed by aggregating temporally stable in-situ soil moisture measurement to a coarser scale (Cosh et al., 2004, 2006; Wang et al. 2008). However, the accuracy of the input observations dictates the performance of these models.

Hydrological models such as HYDRUS (Simunek et al., 1999) and SWAP (van Dam et al., 1997) can be used to address the issue of spatio-temporal discontinuity in the data across different observation scales and obtain reliable soil moisture estimates at the intermediate (field) scale. However, setting up the boundary conditions demands skills and in-depth knowledge of the existing hydroclimatic variables, topography, and material distribution. At fine scales, validation of these models is done by expensive and laborious in-situ measurements and field campaigns. Therefore, the motivation of this study is to address the scale gap in the catchment scale and point scale soil moisture by providing continuous field scale soil moisture measurements at a hectometer scale.

1.3 Objective: Resolving the Gap in Soil Moisture Measurement

Use of CRNS is a novel method to bridge the scale gap between satellite and point scale dataset. The CRNS works on the principle of energy transfer loss due to the inelastic collisions between fast-moving neutrons and the nuclei of hydrogen atoms (Zreda et al., 2008). In nature, hydrogen is most abundant in water molecules consisting of two hydrogen atoms. These atoms reduce the intensity of fast-moving cosmic neutrons through collisions. The difference between no. of incoming and outgoing fast neutrons which is measured by the CRNS sensor provides the no. of slow moving neutrons generated due to inelastic collisions. These measurements are

used to calculate soil moisture in the region. CRNS has performed well across the world in different hydroclimates we find in USA (Zreda et al.; 2012, Franz et al., 2012), Australia (Hawdon et al., 2015), Germany (Baatz et al., 2015) and Italy (Ragab et al., 2017).

The CRNS sensor provides the average soil moisture for a circular area within an approximately 300 m radius which closely mimics the extent of an average agricultural field in Texas. However, the instrument is sensitive to all the hydrogen pools present near the surface, and therefore corrections are required to filter out slow neutron count contributed by soil moisture, from other sources such as near-surface atmospheric moisture (Rosolem et al., 2013), biomass water(Tian et al., 2016), and water present in the soil lattice(Desilets et al., 2010).

The calibration of the CRNS sensor requires upscaling of in-situ data (Baatz et al., 2012; Hawdon et al., 2014). The spatial extent of in–situ samples required for satisfactory calibration depends on the sensitivity of CRNS to measure soil moisture which is inversely proportional distance from the sensor (Baroni et al., 2018) and vegetation cover. A weighting scheme is used to account for this loss of sensitivity (Coopersmith et al., 2014). The existing soil moisture conditions govern the vertical support of a CRNS measurement (10 cm in wet soil to 70 cm in dry soil). However, as it is difficult to pre-ascertain the soil moisture conditions at a site, a strict calibration procedure is employed across the regions. However, as mentioned earlier if the site has high clay content that introduces considerable instrument biases (fig. 2), calibration done using statistical models is unreliable (Mittelbach et al.,2012; Datta et al.,2018).

Neutron counts for the dry soil are used to determine the calibration curve for a site using a texture independent calibration function (Desilets et al., 2010). Generally, radial or

stratified sampling of soil at different depths accompanied by vegetation sampling is carried out during different seasons to capture the entire relationship between soil type and neutron count. Multiple field campaigns pose a challenge if the sites are far apart or have a rigid soil matrix to make any digging and in situ data collection possible.

A simple water budget or numerical model can be used for calibration (Lv et al., 2014; Schreiner-McGraw et al., 2016).Use of Hydrus 1D for calibration has shown significant improvements in the sensor performance (Lv et al., 2014). However, it must be noted that in numerical modeling at a continuous timescale, vegetation water content is no longer a constant hydrogen pool and should be considered in the calibration studies. Moreover, Hydrus 1D ignores the effect of topography and land surface material distribution which contributes to the movement of water in the system and should be studied if a continuous calibration procedure is adopted. Schreiner-McGraw et al.(2016) calibrated the CRNS sensors using water budget equation. They compared CRNS and in-situ TDR probes by showing improvements in evaporative fluxes obtained using a piecewise linear regression model which uses soil moisture measurements as inputs (Rodríguez-Iturbe et al., 2007).Eddy Covariance Towers, which are a non-invasive instrument to determine evapotranspiration (ET), can be used for validation of different ET products (Jia et al., 2012; Saadi et al., 2018). Since, the in-situ measurements are not performing well(Fig. 2), we can use satellite ET to set a baseline for performance evaluation of CRNS derived ET (CRNS-ET).Therefore, in this study:

i) We use a 2-dimensional sub-surface model, Hydrus2D, to incorporate the effect of topography and spatially distributed soil properties in the calibration of CRNS sensors. The sensors were calibrated under different vegetation covers and management practices using

effective soil hydraulic parameters for different months to account for seasonality and different vegetation conditions.

ii) We validate the (calibrated) soil moisture values against two independent variables – 1) gravimetric soil moisture from field campaigns and 2) ET from eddy covariance towers and Landsat 8 thermal sensors. Validation using a state variable and an atmospheric forcing is done to diminish the possible bias introduced by invasive in-situ soil moisture data collection.

CHAPTER II

CALIBRATION OF CRNS USING MODEL BASED APPROACH

In this chapter we discuss the calibration the CRNS in mixed land use/land cover by using Hydrus 1D and Hydrus 2D simulations in Southeastern Texas. The chapter addresses the difficulty in measurement of in-situ dataset for calibration of CRNS in compacted soils with high clay content.

2.1 Study Area

As part of Texas Water Observatory (TWO) initiative, CRNS sensors were installed at three sites with different land covers in the Brazos River Basin (Figure 1). The first site is part of a USDA facility located near Riesel, Texas (31°28'09.6"N 96°53'11.2"W). The site is a traditionally managed agriculture field at an elevation of approximately 173m and slope of about 1.2^{o}. The total annual rainfall at the site is 914 mm and mean maximum and minimum temperature 25.1°C and 12.8°C respectively (Mohanty et al., 2015). The primary crop planted is corn, and it covers an area 5.82 hectares. Three soil nodes (SN1, SN2, and SN3) with five electromagnetic reflectometry-based probes each at different depths (5, 15, 20, 75, 100 cm) are installed at the site (Table 1). The CRNS is in the middle of the field at node SN1. The major soil types are Houston Black clay and Heiden clay.

The second site located near Thrall, Texas and is a part of Stiles Farm Foundation (30°37'03.5"N 97°17'37.8"W). The site represents unmanaged prairie with an area of about 203 hectares and a gentle slope of 1.2^{o}. The site's elevation is approximately 157 m and it receives a total annual rainfall of about 889 mm. The mean annual maximum and minimum temperature

at the site is 25.6°C and 13.3°C respectively (Mohanty et al., 2015). This site has two soil nodes with electromagnetic probes at 5 similar depths as the Riesel site. The CRNS is installed at one of soil nodes at the site. The significant soils present in the study area are Houston Black clay, Heiden clay, and Altoga silty clay loam.

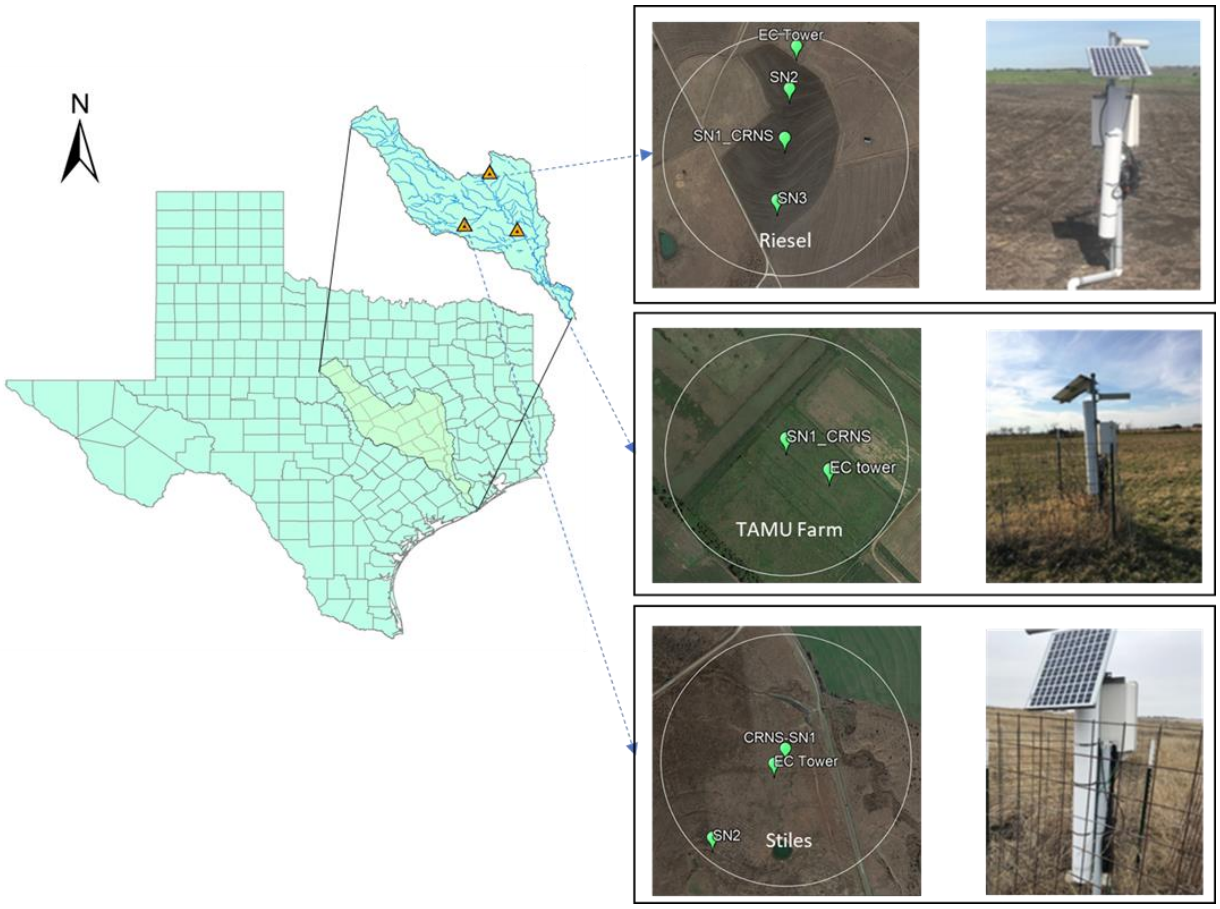

Figure 1 a) location of three sites i.e. Riesel traditional farm, TFPR and Stiles Farm in the Lower Brazos River basin b) Circular footprint of CRNS sensor c) CRNS sensors at the sites

The third site, Texas A&M Prairie Farm (TFPR) is part of the Texas A&M research farm (TFPR) (30°33'07.7"N 96°25'32.2"W). It is a managed prairie site with an elevation of about 73m and has a flat terrain. Total annual rainfall is 991mm, and the average temperature is range is 26.0°C - 13.9°C (Mohanty et al., 2015). The CRNS is installed on the only soil node present at the site. The major soils at the site are Weswood silty clay loam, Weswood silt loam, Yahola very fine sandy loam, Belk clay, and Rotex clay.

All sites are identically instrumented (Table 1) notably with eddy covariance towers, soil nodes, tipping bucket rain gauges and phenocams to monitor atmospheric variables and vegetation growth. For Stiles we collected additional rainfall dataset using a USGS raingauge nearby.

Table 1 List of TWO Instruments used in the present study

Instrument	Company	Variable	Notation	Footprint	Depth
CS655 12cm Water Content Reflectometer		Soil Moisture	SN1, SN2, SN3 at Riesel SN1, SN2, SN3at Stiles Farm SN at Tamu Farm		5cm, 15cm, 30cm, 75cm, 100cm
CRS-1000 Cosmic Ray Soil Moisture Observation System		Soil Moisture		300m	Variable (10cm-70cm)
Eddy Covariance Measurement Station	Campbell Scientific	Latent Energy Relative Humidity Wind Speed& Direction Atmospheric Pressure Radiation		75m	
MPS6		Metric Potential	SN1, SN2, SN3 at Riesel SN1 and SN2 at Stiles Farm SN at Tamu Farm		5cm, 15cm, 30cm, 75cm, 100cm
Tipping Bucket Raingauge		Precipitation			

As discussed earlier, the higher clay content distorted the signals from the electromagnetic probes (Fig. 2). At Riesel, two soil nodes (SN) and at stiles farm one soil node has overestimated soil water contents during the drying period. At TFPR, one of the five sensors has shown lower soil moisture variability throughout the study period.

Figure 2 Uncalibrated CS 655 signal at a) Riesel SN1 b) Riesel SN2 c) Stiles SN1 d) TFPR SN. The values are overestimated due to high clay content

The sites have different weather conditions contributing towards varying CRNS' response. Therefore, we corrected the raw neutron count coming from the sensors to remove the effect of different hydroclimates.

2.2 Raw Neutron Count Correction

The atmospheric water vapor influences the neutron count of a CRNS system. Rosolem et al.(2013)proposed a correction factor (C_{wv}, eq. 1) which considers the relative humidity, temperature, air pressure, and near-surface moisture. (1)

$$C_{wv} = 1 + 0.0054 \triangle p_{v0}$$

Where $\triangle \mathrm{p_{v0}} = (\mathrm{p_{v0}} - \mathrm{p_{v0}}^{\mathrm{ref}})$ is the difference between absolute humidity and the absolute relative humidity in (gm^{-3}).Changes in atmospheric pressure can cause the attenuation of cosmic ray flux since the air mass is changing (Bogena et al., 2013). Therefore, we perform a correction$(\mathrm{C_p}, \mathrm{eq.}\ 2)$ for the changes in near-surface air pressure.

(2)

$$C_p = e^{\left(\frac{Pi-Po}{L}\right)}$$

Where P_i is the current air pressure and P_o is the reference air pressure at the site. L is the attenuation length of neutrons (gcm^{-2}) at the site.

Additionally, the neutron count is corrected for incoming neutron flux$(\mathrm{C_I}, \mathrm{eq.}\ 3)$ to filter out the signals from neutrons unaffected by the hydrogen molecules (Simpson et al., 2000; Hawdon et al., 2014). Data for neutron flux intensity is obtained from the closest neutron monitoring station located in the MOISST Oklahoma site.

$$C_I = \frac{I_m}{I_{ref}} \tag{3}$$

Here $\mathrm{I_m}$is the current neutron counting rate whereas $\mathrm{I_{ref}}$ reference neutron counting rate at the Oklahoma Site. There were gaps and inconsistencies in the dataset which were interpolated using the cubic spline function. While performing corrections, the cutoff rigidity C_S based on the geomagnetic latitude is also considered (Smart and Shea 2001).The corrections are applied to determine the corrected neutron count N (eq. 4) using the raw neutron count from the sensor N_{raw},

$$N = N_{raw}\frac{C_P C_{wv}}{C_I C_S} \tag{4}$$

N obtained from equation 4 must be translated to soil moisture either using in-situ measurements or numerically modeled soil moisture.

2.3 Area Average Soil Moisture Content using Numerical Modeling

For numerical simulation of soil moisture dynamics in the system, we used the Hydrus_2D model (Simunek et al., 1999). It uses two-dimensional Richard's equation to simulate soil moisture movement in the unsaturated zone (eq 5).

$$\frac{\partial\theta}{\partial t} = \frac{\partial}{\partial x}\left[K(h)\frac{\partial h}{\partial x}\right] + \frac{\partial}{\partial z}\left[K(h)\frac{\partial h}{\partial z} + K(h)\right] - S \tag{5}$$

Where θ is soil moisture, $\mathrm{K(h)}$ is the unsaturated hydraulic conductivity function with respect to pressure head h and S is a sink term. van Genuchten-Maulem curve(van Genuchten, 1985) was used to determine the soil hydraulic retention function (eq. 6),

$$S_e(h) = \frac{\theta_h - \theta_r}{\theta_s - \theta_r} = \begin{cases} [1 + (|\,\alpha h\,|)^n]^{-m} & h < 0 \\ 1 & h \geq 0 \end{cases} \tag{6}$$

$$K(S_e) = K_s S_e^l [1 - (1 - S_e^{1/m})^m]^2$$

Where$\mathrm{S_e(h)}$ is effective saturation, θ_s is saturated moisture content, θ_r is residual moisture content, $\mathrm{K_s}$ is saturated hydraulic conductivity, α is the inverse of air entry pressure, n and m are shape parameters.

2.3.1 Inverse Modeling of Soil Hydraulic Parameters using Hydrus 1D

First, we performed inverse modeling at the soil nodes (SN) to determine soil hydraulic parameters for each individual site/location using Hydrus1D. We used shuffled complex evolution algorithm (SCE-UA) to carry out global optimization of the parameters (Duanet et al., 1993). SCE-UA has been widely used for inverse modeling of soil hydraulic parameters (Guo et al., 2013; Durner et al., 2008). Using the algorithm, we maximized the coefficient of determination (R^2) at each soil node by adjusting the parameters. In accordance with CRNS' penetration depth (eq. 8), simulation was carried out for top 250-300 mm soil profile.

Root water uptake was simulated through Feddes Curve parameters (Feddes et al., 1974). We used Landsat 7'sNormalized Difference Vegetation Index (NDVI) as a proxy for vegetation water content because of its high spatial resolution (30 m) and good temporal resolution (16 days). We calculated two sets of parameters for low and high vegetation water content at each soil node. The availability of auxiliary dataset determined the period of simulation at each location, and the timestep was 30 min. It may be noted that we calculated three sets of parameters (Bare soil, Low Vegetation, High Vegetation) for each soil node at Riesel.

We fixed the surface boundary conditions as atmospheric with surface runoff, using the ET data from the eddy covariance towers and precipitation from the rain gauges. We partitioned ET using suggested E/ET ratio (Kool et al., 2014). Since the water table is much deeper than the soil profile in all the locations, we kept free drainage as the bottom boundary condition. We kept the profile discretization at a single node every three 3cm. We calculated

van Genuchten-Maulem parameters for the months March, May, and July at Riesel, March, and May at Stiles farm and, May and July at TFPR (Table 2) accounting for any soil structural changes due to changing vegetation cover.

We also determined soil hydraulic parameters using ROSETTA (Schaap et al. 2001). We obtained the soil textural classification from National Cooperative Soil Survey Characterization Data using ROSETTA.

Table 2 Soil Hydraulic parameters from ROSETTA

Site	θ_r m^3m^{-3}	θ_s m^3m^{-3}	α	n 1/m	K_s m/day	l
Riesel	0.09	0.49	1.36	1.4	0.12	0.5
Stiles	0.09	0.48	1.45	1.39	0.11	0.5
TFPR	0.1	0.51	1.9	1.24	0.09	0.5

2.3.2 Simulation of Soil Moisture Content using Hydrus 2D

To simulate soil moisture conditions in a cross section of the CRNS footprint, we cut a transect of length 600mthrough the field (Fig. 3) such that it included all soil nodes in the study area. The simulation was carried at a timestep of 360 min in a 600 m long and 0.3 m deep soil profile. We calculated the average slope utilizing a digital elevation model (~30m spatial resolution) prepared from National Elevation Dataset (NED) 2013. We distributed the material in the profile according to the electrical conductance (EC) dataset from the field campaigns (Fig. 4).We considered atmospheric boundary conditions on the surface and free drainage along the bottom and sides of the profile.

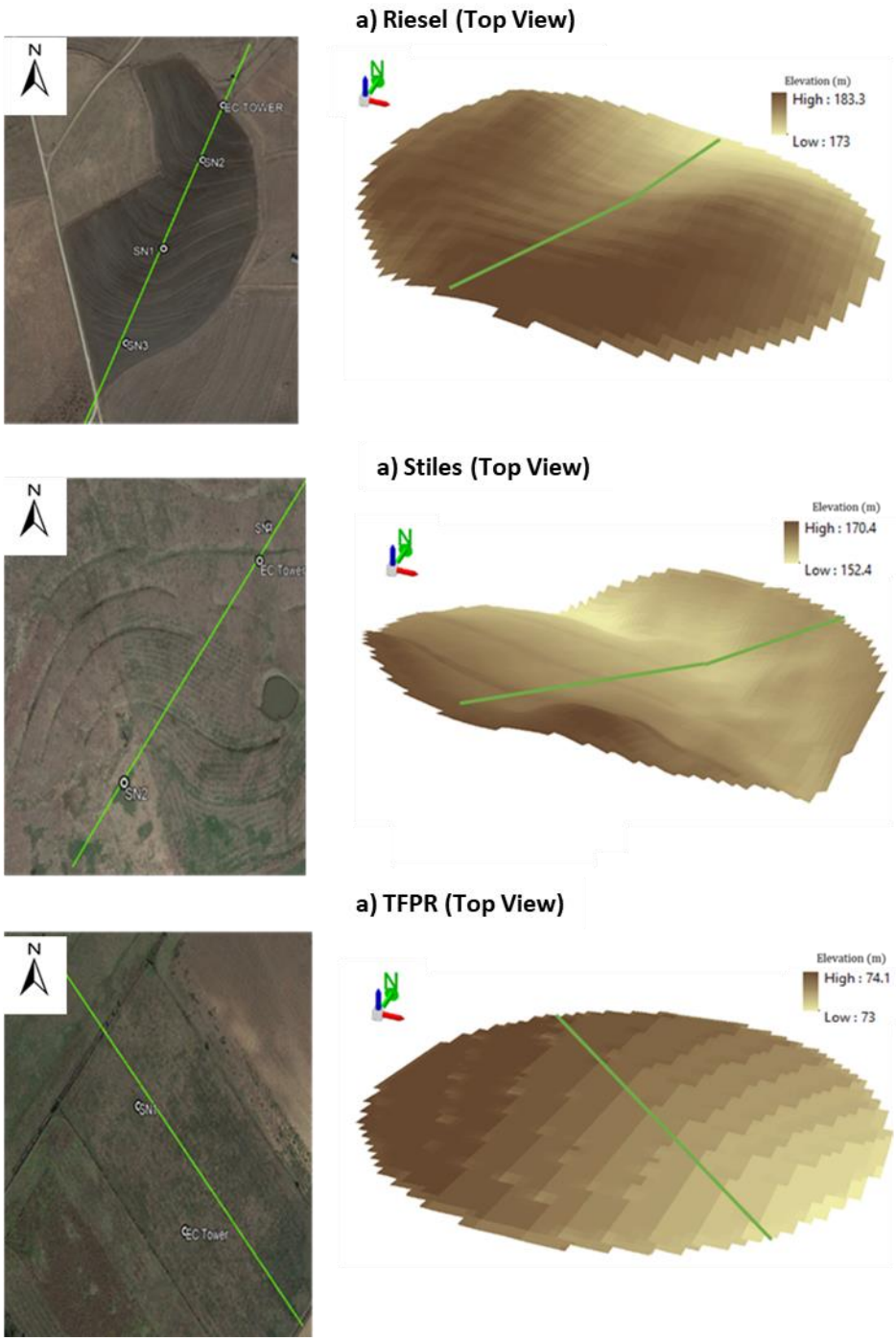

Figure 3. Top view of profile and 3D elevation of a) Riesel, b) Stiles Farm and c) TFPR. Green Transect represents the cross section where the soil moisture is simulated

To set up the initial conditions, we assumed a linear distribution of soil moisture according to the depth, with top and bottom soil moisture contents obtained from the in-situ probes. We simulated the soil moisture content in the months of March, May, and July at Riesel, March, and May at Stiles farm and, May and July at TFPR (Fig. 14). After obtaining the soil moisture distribution across the transect cross section, we determined the profile average soil moisture θ_v in the CRNS footprint. The θ_v is then used to calibrate the CRNS.

2.4 Calibration of CRNS

The final neutron count is calibrated to soil moisture using the modified calibration function given by equation 7(Franz et al., 2013; Hawdon et al., 2014).

$$\theta_V = \left(\frac{0.808}{\left(\frac{N}{N_o}\right) - 0.372} - 0.115 - w_{lt} - w_{som} \right) \rho_{bd} \quad (7)$$

Where θ_v (m^3/m^3)is the volumetric soil moisture,$\rho_{bd}$is bulk density,N is corrected neutron count, N_o is the site specific neutron count for completely dried soil, w_{lt} is the lattice water contained and w_{som} is water present in organic matter.Avery et al., (2013), has provided thew_{lt} distribution for contiguous United States. We used Web Soil Survey (WSS) to gather$\rho_{bd}$and w_{som}datafor all the sites. The penetration depth, z (cm) of the CRNS is given by Franz et al., 2013 (eq. 8).

$$z = \frac{5.8}{\frac{\rho_{bd}}{\rho_w}(w_{lt}+w_{soc})+\theta_v+0.0829} \quad (8)$$

We optimized the value of N_o by minimizing the least square error between numerically modeled soil moisture and the soil moisture obtained from the calibration function. In addition

to regular value of N_o, we subsetted the data using NDVI as a proxy for vegetation water content and calculated individual N_o for the high and low NDVI scenario (Table 3).

2.5 Results

2.5.1 Correction of Neutron Count

Figure 4&5 shows the atmospheric, pressure and neutron intensity corrections for the three sites. The average neutron count rates increased in all three sites after application of the neutron correction factor (Fig. 6). Figure7 illustrates the reduction in uncertainty in all the three sites. The average corrected neutron count rate at Riesel, Stiles and TFPR is 768 Ch^{-1}, 726 Ch^{-1} and 795 is Ch^{-1} respectively whereas raw neutron count rate at the sites are 788 Ch^{-1}, 707 Ch^{-1} and 658 Ch^{-1}.

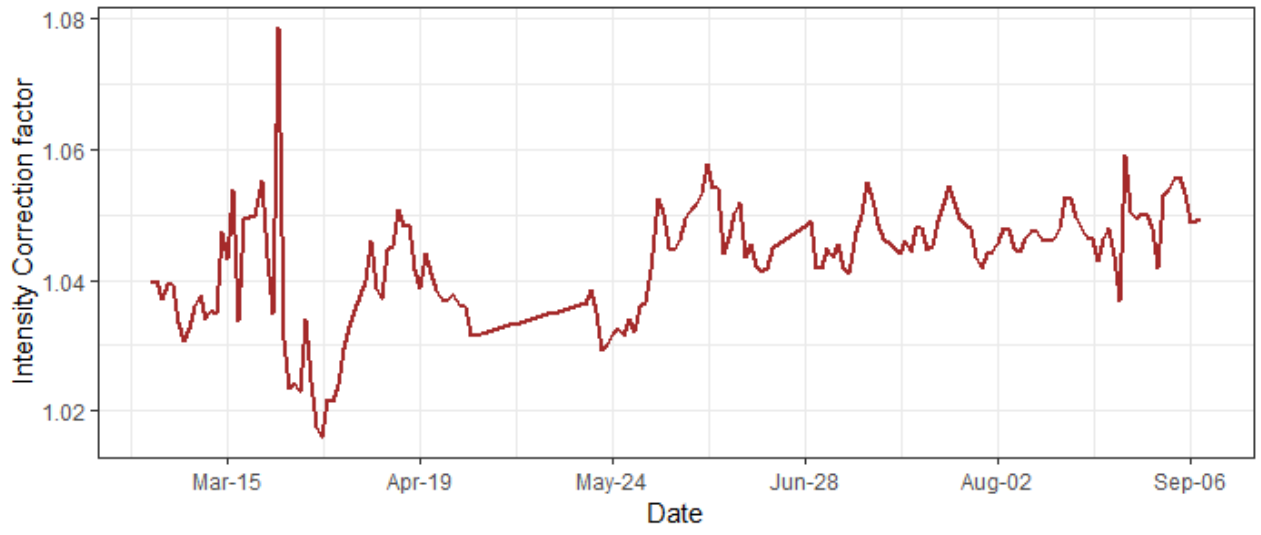

Figure 4 Cosmic ray intensity correction factor at MOISST, Oklahoma site

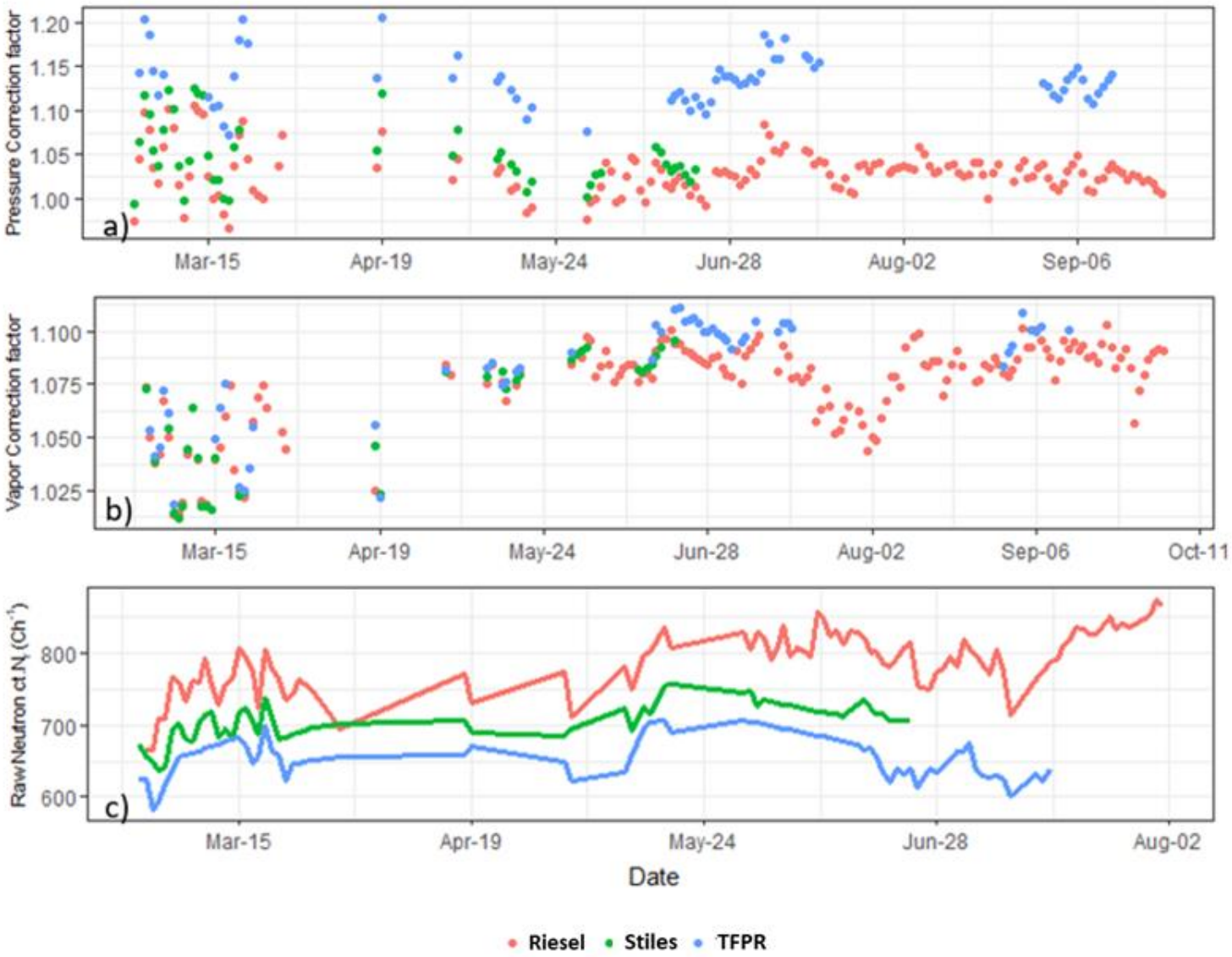

Figure 5 Time series of a) atmospheric pressure correction (Cp) b) water vapor correction (Cwv) and c) raw neutron count (Nr) at the three sites

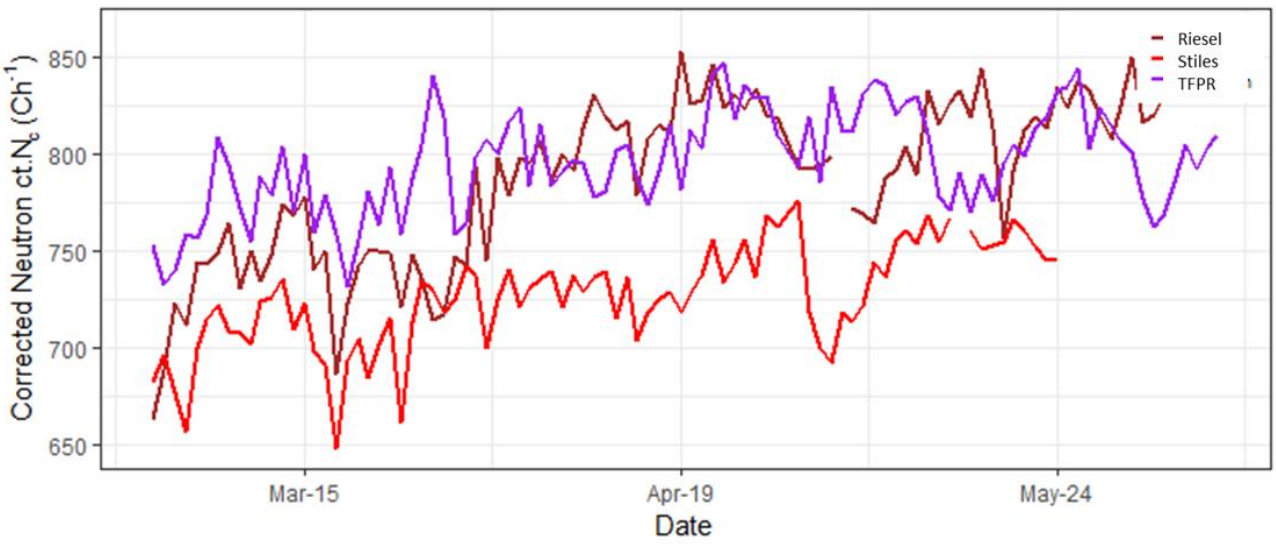

Figure 6 Time series of corrected neutron Count (Nc)

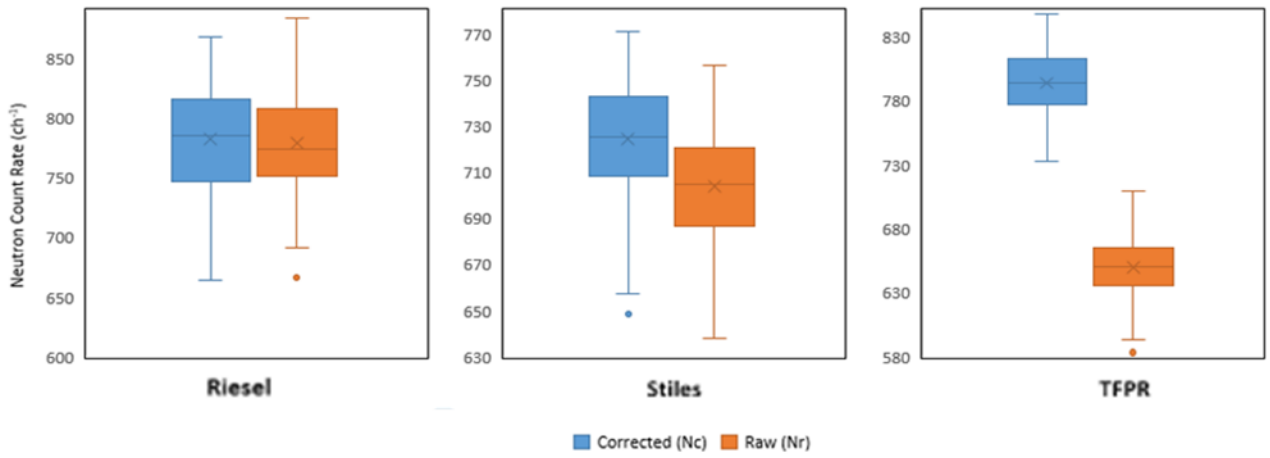

Figure 7 Comparison between corrected neutron count rate and raw neutron count rate in a) Riesel b) Stiles farm and c) TFPR

2.5.2 Numerical Modeling of Soil Moisture Distribution

Table 2 shows the optimized soil hydraulic parameters for the different vegetation covers as obtained from inverse modeling. For the ease of computation, we calculated effective

parameters for the whole soil profile without considering the changes in material as we go down the profile. Figure 8 shows the simulation results for different months.

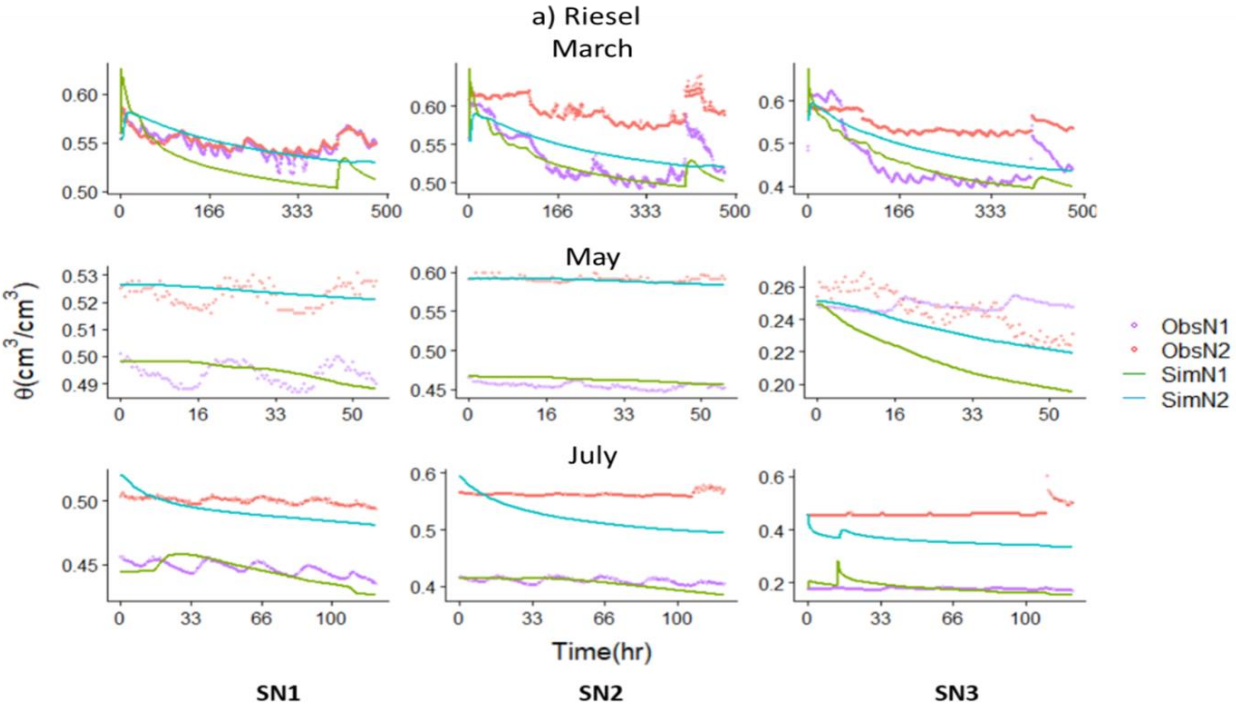

Figure 8 Comparison between simulated soil moisture and observed soil moisture during different time periods in a) Riesel b) Stiles farm and c) TFPR

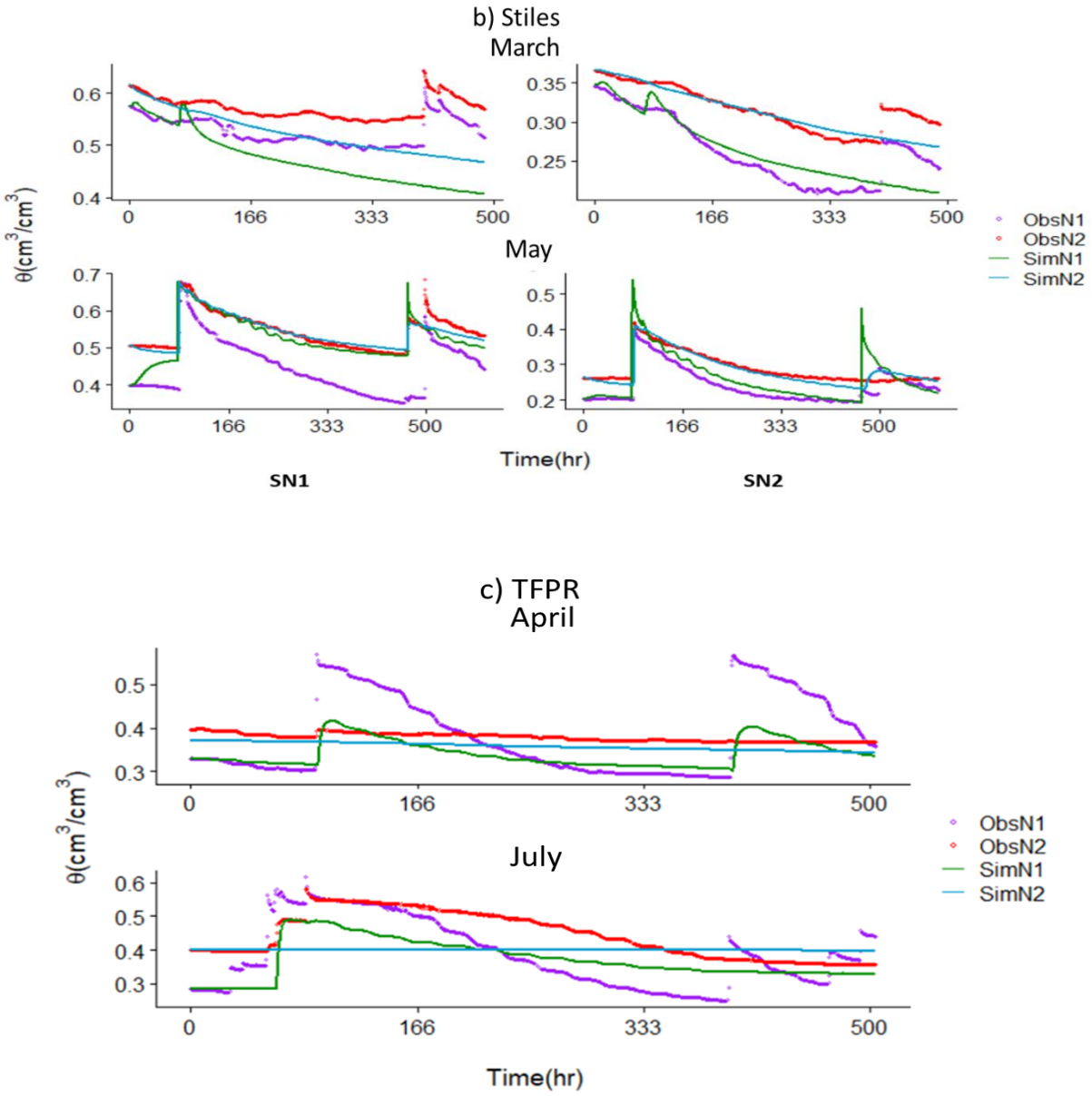

Figure 8 Continued.

As discussed earlier (Fig. 2), there seems to be an overestimation of field observed data in most of the soil nodes due to high clay content. Therefore, compared to ROSETTA parameters (Table 2) we noted higher than expected estimates of θ_s and θ_r (Table 3). Except for summer months in Riesel we ran the model for long periods of time at a small timestep of 30

min. As we had dataset for few months, to capture temporally short weather events, we kept the timestep small and did not average the values to a daily timescale. Hydrus 1D is less suitable for modeling transpiration driven long term fluctuation (Chen et al., 2014).Therefore, the results could not capture the peak values but adequately simulated the recession limb (Fig. 8). However, the low Root Mean Square Error (RMSE) values (Table 3) suggest that the model was able to account for the total water balance during the simulation run. At Stiles, the precipitation values may have not been reflected in the simulation run as they were obtained from the Raingauge at a different site. The optimization algorithm SCE-UA was driven by the R^2 values between observed and the simulated dataset. We got acceptable R^2 for SN3 in Riesel and SN2 in Stiles, where the performance of the TDR probes is seemingly not affected by the clay content. We have calculated effective parameters only for the calibration of CRNS dataset. Generally, the value of soil hydraulic parameters does not change with time. Hence, values obtained in this study should not be used for long term hydrological studies in the region.

Table 3 Effective soil hydraulic parameters for the three sites during different months

Site	Soil Node	Month	θ_r	θ_s	α	n	K_{sat}	l	R^2	RMSE
			m^3/m^3	m^3/m^3	1/m		m/day			m^3/m^3
Riesel	SN1	March	0.12	0.63	4.4	1.1	0.29	0.51	0.56	0.02
	SN2		0.12	0.65	3.6	1.1	0.69	0.52	0.58	0.03
	SN3		0.1	0.68	6.1	1.28	0.36	0.5	0.66	0.05
	SN1	May	0.1	0.63	22	1.17	0.26	0.5	0.32	0.01
	SN2		0.09	0.63	41	1.17	0.03	0.5	0.45	0.01
	SN3		0.11	0.61	33	1.18	0.26	0.49	0.54	0.01
	SN1	June	0.11	0.52	21	1.18	0.09	0.49	0.55	0.02
	SN2		0.09	0.54	30	1.65	0.01	0.51	0.52	0.07
	SN3		0.1	0.3	40	1.43	2.35	0.5	0.51	0.06
Stiles	SN1	March	0.12	0.68	8.6	1.38	0.07	0.51	0.51	0.07
	SN2		0.06	0.68	1.0	1.8	0.27	0.51	0.77	0.02
	SN1	May	0.11	0.55	23	1.11	1.09	0.5	0.71	0.06
	SN2		0.09	0.55	2.1	1.73	0.13	0.52	0.83	0.03
TFPR	SN1	April	0.09	0.67	1.5	1.23	0.17	0.52	0.44	0.06
	SN1	July	0.12	0.58	33	1.1	1.11	0.49	0.4	0.07

Figure 9 shows the water content in the cross section. We use the information to calculate the average value of volumetric water content in the cross section during the simulation period. Slope in the profile and root zone distribution, ensured that the model was driven by topography, ET and root water uptake in Riesel and Stiles (Fig. 9). Therefore, we can see considerable variation in soil moisture as the time progresses. Fig. 9 shows Riesel and Stiles with distinct wetting fronts. At Stiles there is a substantial difference between the soil hydraulic parameters. SN2 at Stiles is at a higher elevation and the soil moisture drawdown is high. Therefore, the profile looks different and we can see a transition zone in the middle. TFPR had a flat profile and only ET, root water uptake and drainage was responsible for water loss in TFPR. Therefore, the spatial variability seems to be conserved in TFPR for long periods of time. Like the inverse solution, Hydrus 2D simulations were unable to capture the peak values but could simulate the recession limb.

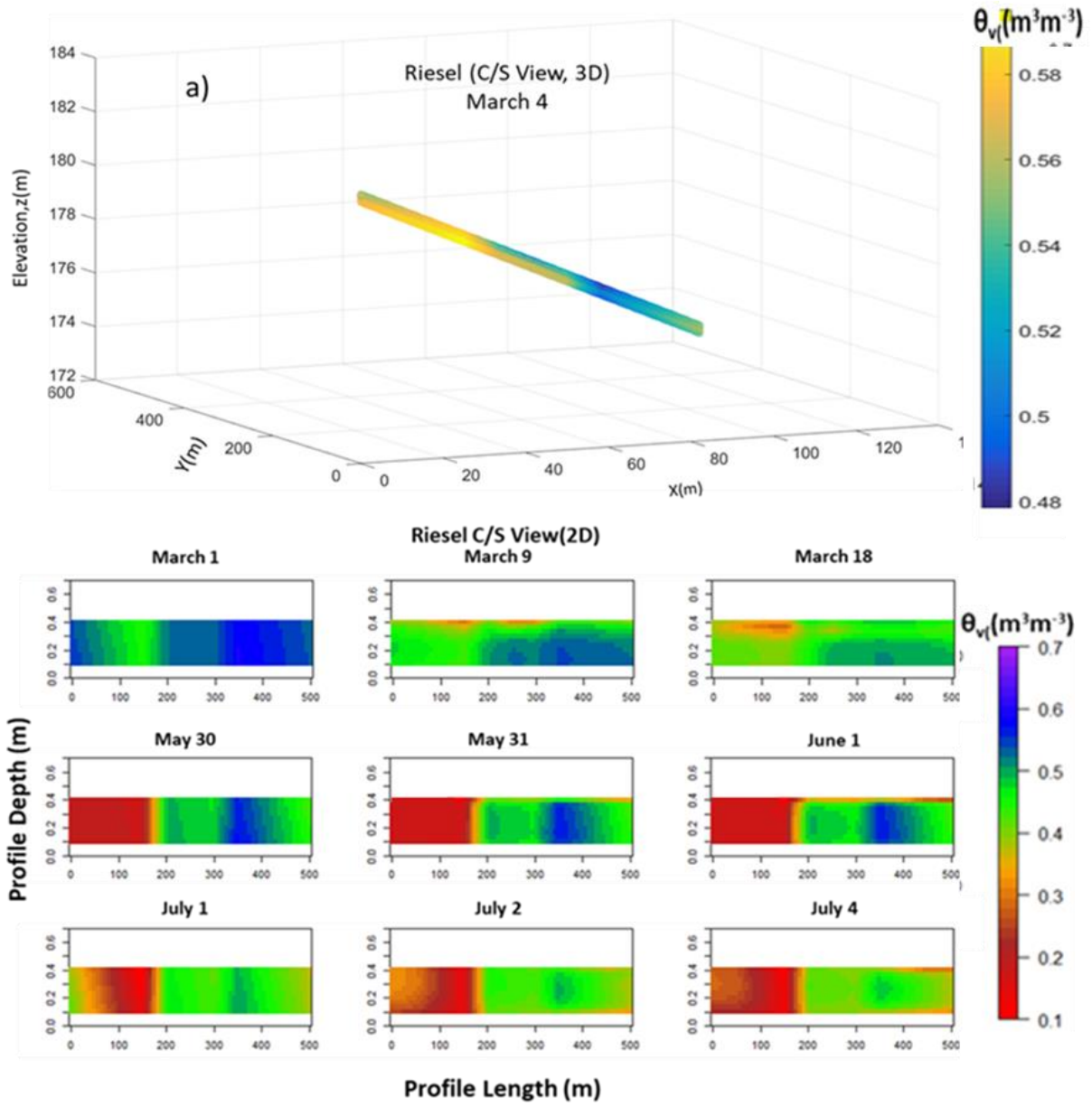

Figure 9 Soil Moisture distribution in the profile cross section(c/s) at a) Riesel, b) Stiles and c) TFPR obtained using Hydrus 2D simulations. TFPR has a straight profile as the slope is 0^{o}.

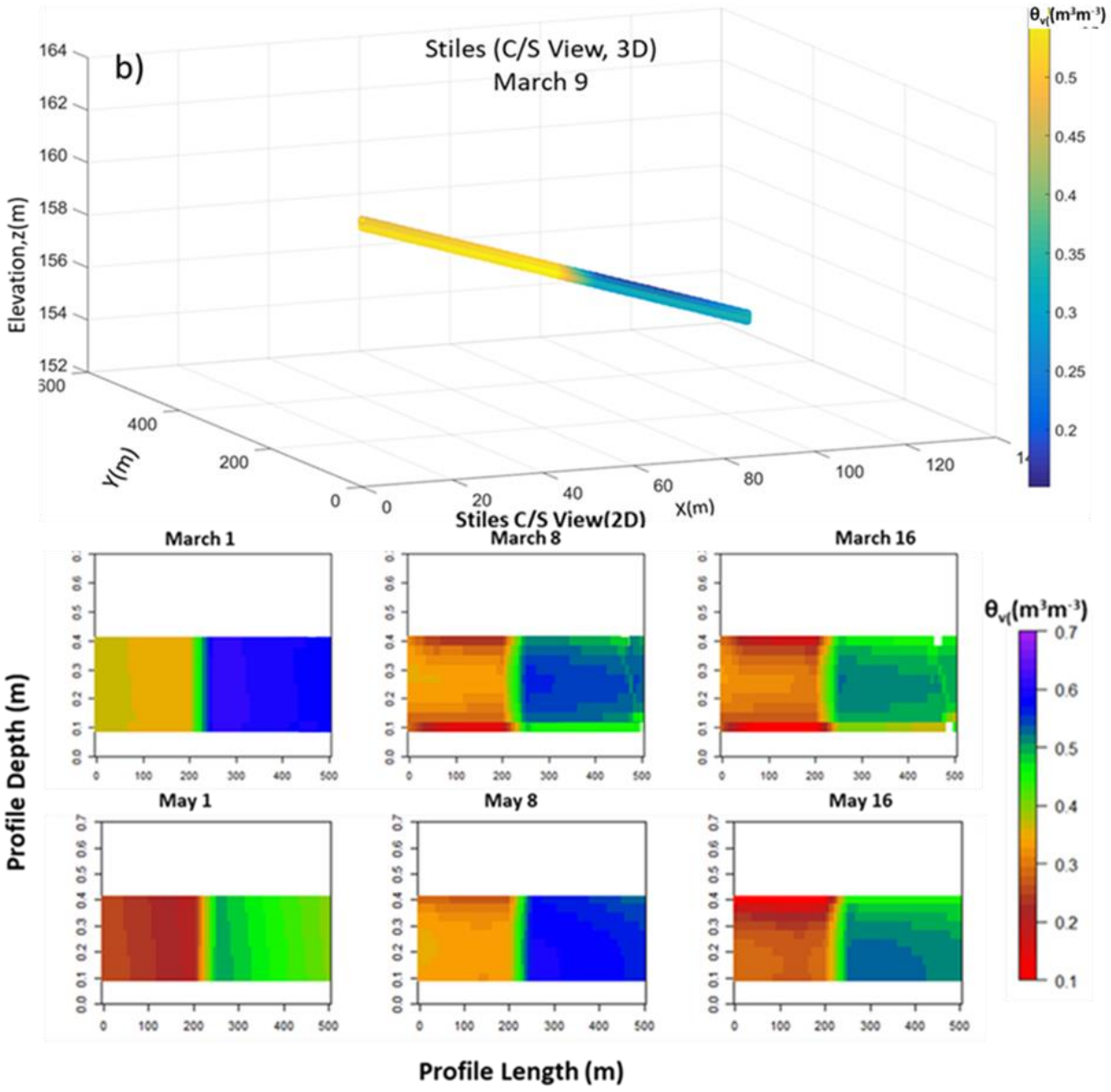

Figure 9 Continued.

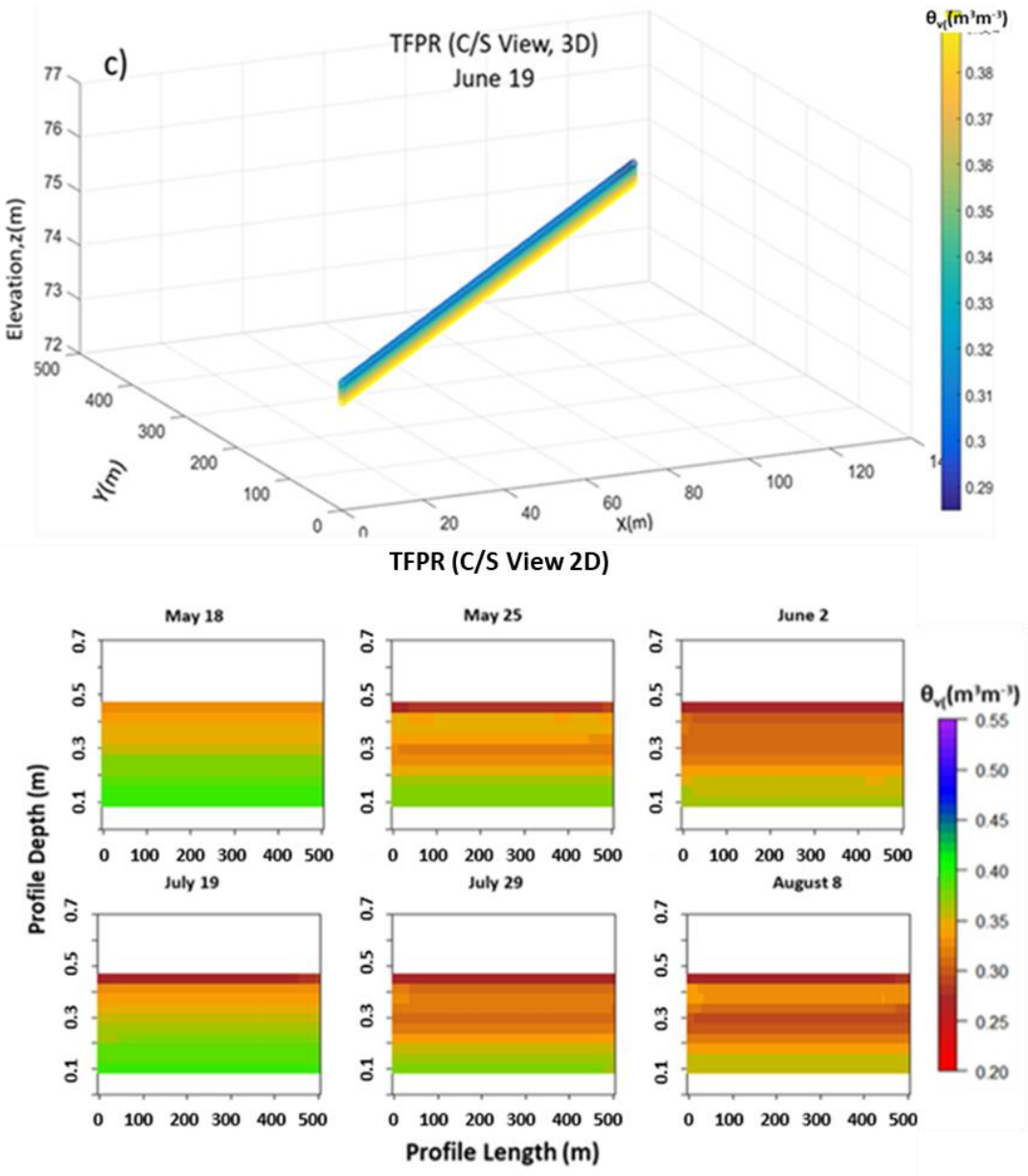

Figure 9 Continued.

2.5.3 Calibration of CRNS

We optimized the value of the calibration parameter N_o for different values of NDVI at all the three sites by minimizing the RMSE between profile average volumetric soil moisture and soil moisture simulated using equation 7 (Fig. 10). Table 4 illustrates the performance of calibration and validation. The RMSE for calibration was slightly better than the validation. We observed low RMSE of (0.04-0.06 m^3m^{-3}) for calibration conducted during high NDVI scenario. At Riesel, for the bare soil or low vegetation scenario, the model-based calibration approach produced poorer results (RMSE=0.12 m^3m^{-3}). This may be due to the tillage performed before seeding which disrupted the topsoil matrix, hence increasing K_s (Reynolds et al., 1995).

Table 4 NDVI dependent CRNS Calibration Parameter, N_o at the three sites

Site	NDVI Category	W_{lt} m^3/m^3	ρ_{bd} g/cm^3	N_o Count/hr	RMSE Calibration m^3/m^3	RMSE Validation m^3/m^3
Riesel	All	0.03	1.33	1386	0.12	0.11
	High	0.03	1.33	1482	0.066	0.041
	Low	0.03	1.33	1392	0.12	0.11
Stiles	All	0.03	1.3	1338	0.066	0.078
	High	0.03	1.3	1290	0.041	0.046
	Low	0.03	1.3	1332	0.067	0.07
TFPR	All	0.03	1.4	1206	0.041	0.044
	High	0.03	1.4	1188	0.042	0.06
	Low	0.03	1.4	1206	0.042	0.039

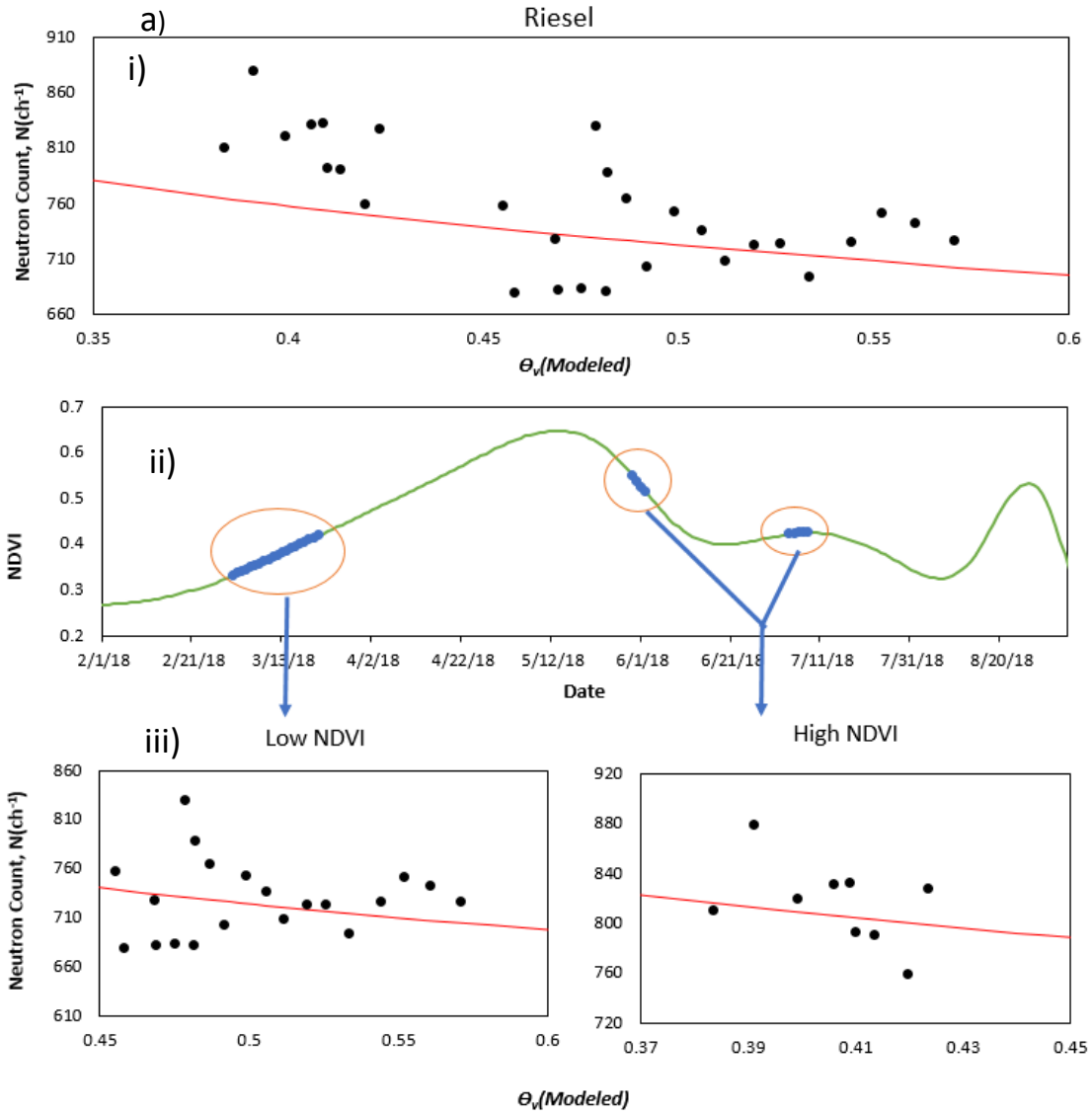

Figure 10 Relationship between Neutron Counting rate N in the CRNS (ch-1) and Soil moisture (θ_v) for a) Riesel, b) Stile and c) TFPR. Here i) N-θ_v relationship from the NDVI independent estimation of calibration parameter No ii) is the Time series of NDVI and iii) N-θ_v relationship from the NDVI dependent estimation of calibration parameter N_o

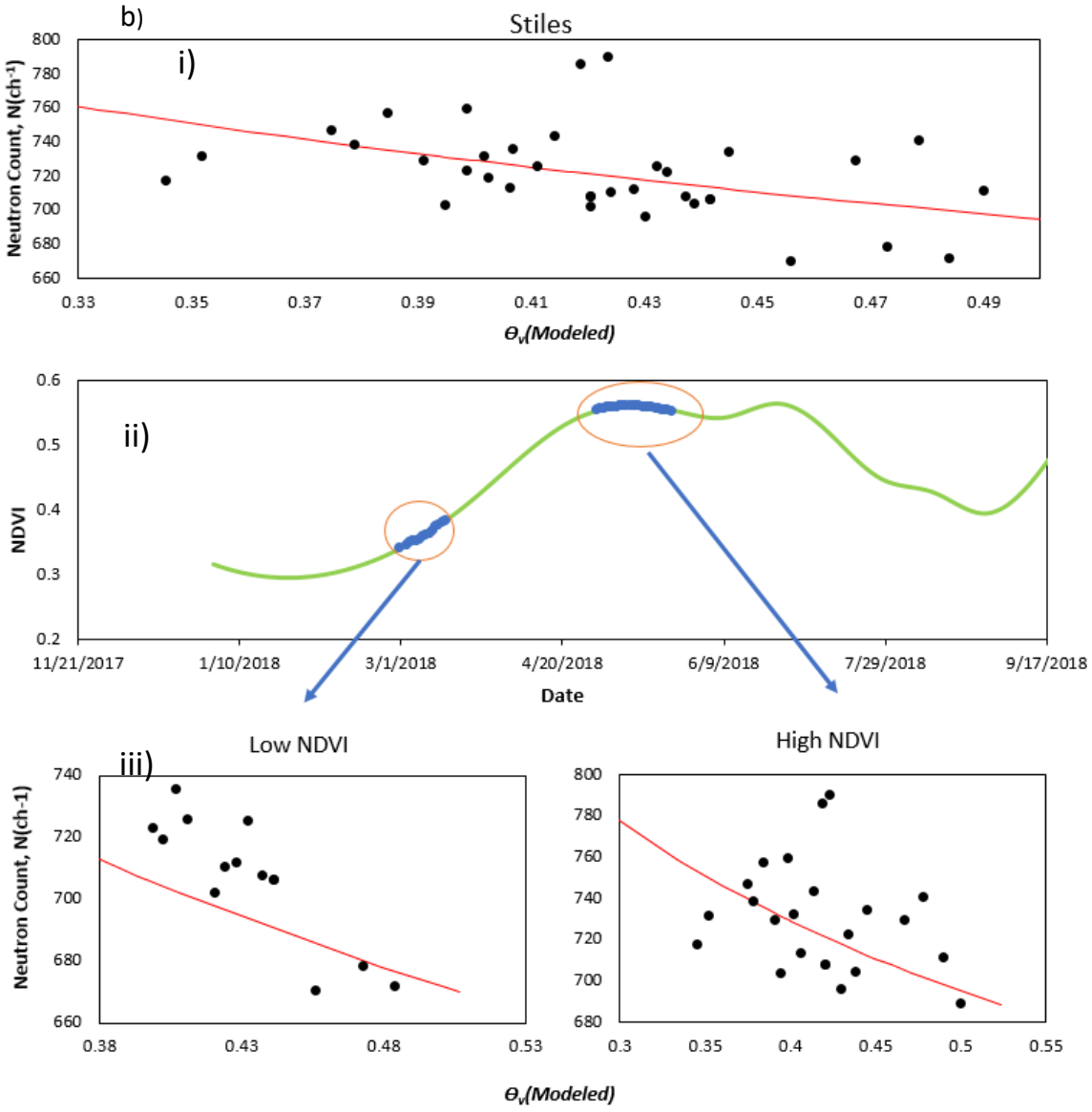

Figure 10 Continued.

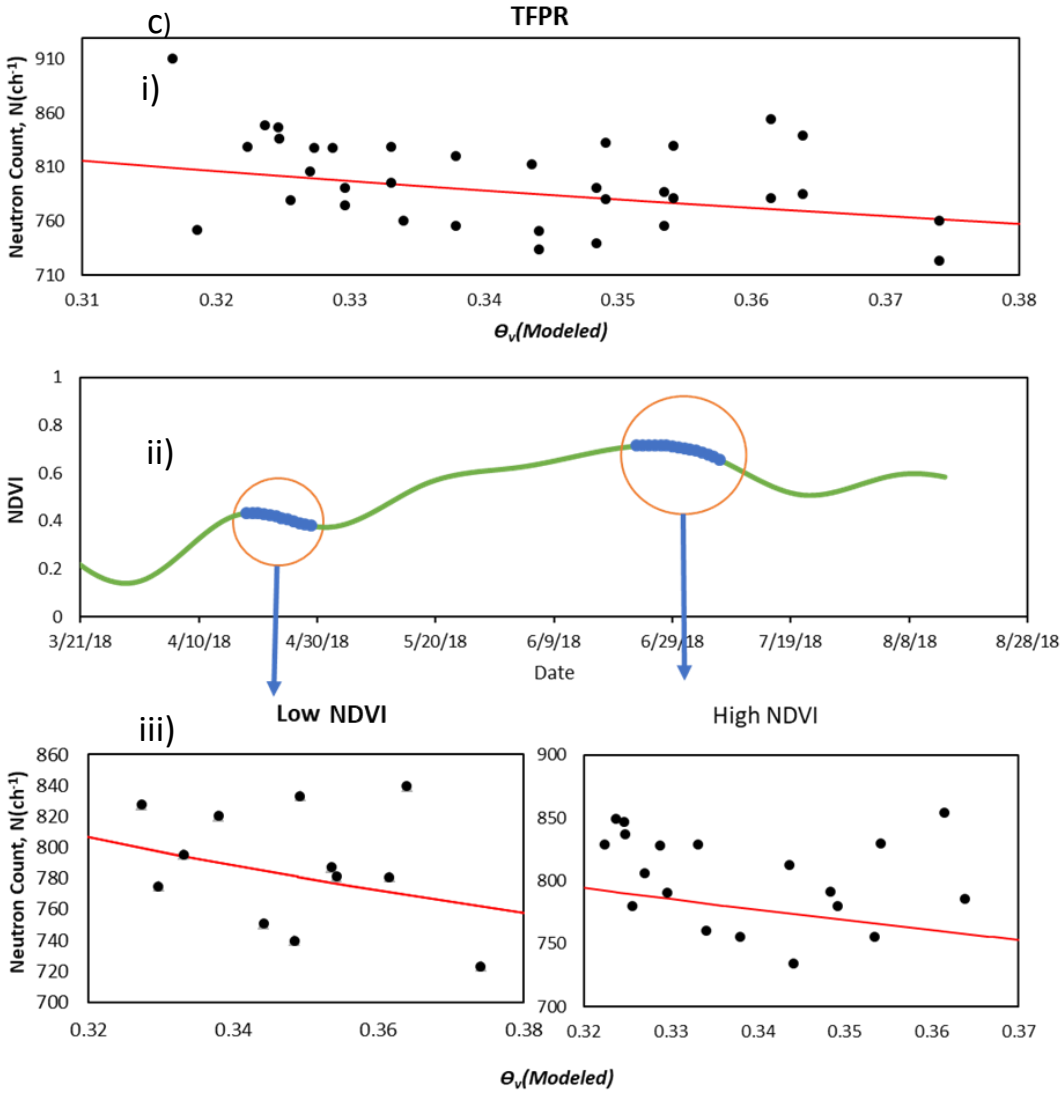

Figure 10 Continued.

Figure 11 shows the vertical support of CRNS calculated using equation 8. As we can see due to perennially high moisture content, the vertical support depths at the three sites is between 10 cm – 15 cm (Fig. 11). As the mean modeled soil moisture is high at the three sites,

the sensing depth is shallow. Therefore, for calibration of the CRNS in similar soils, running the model at shallower depths is sufficient.

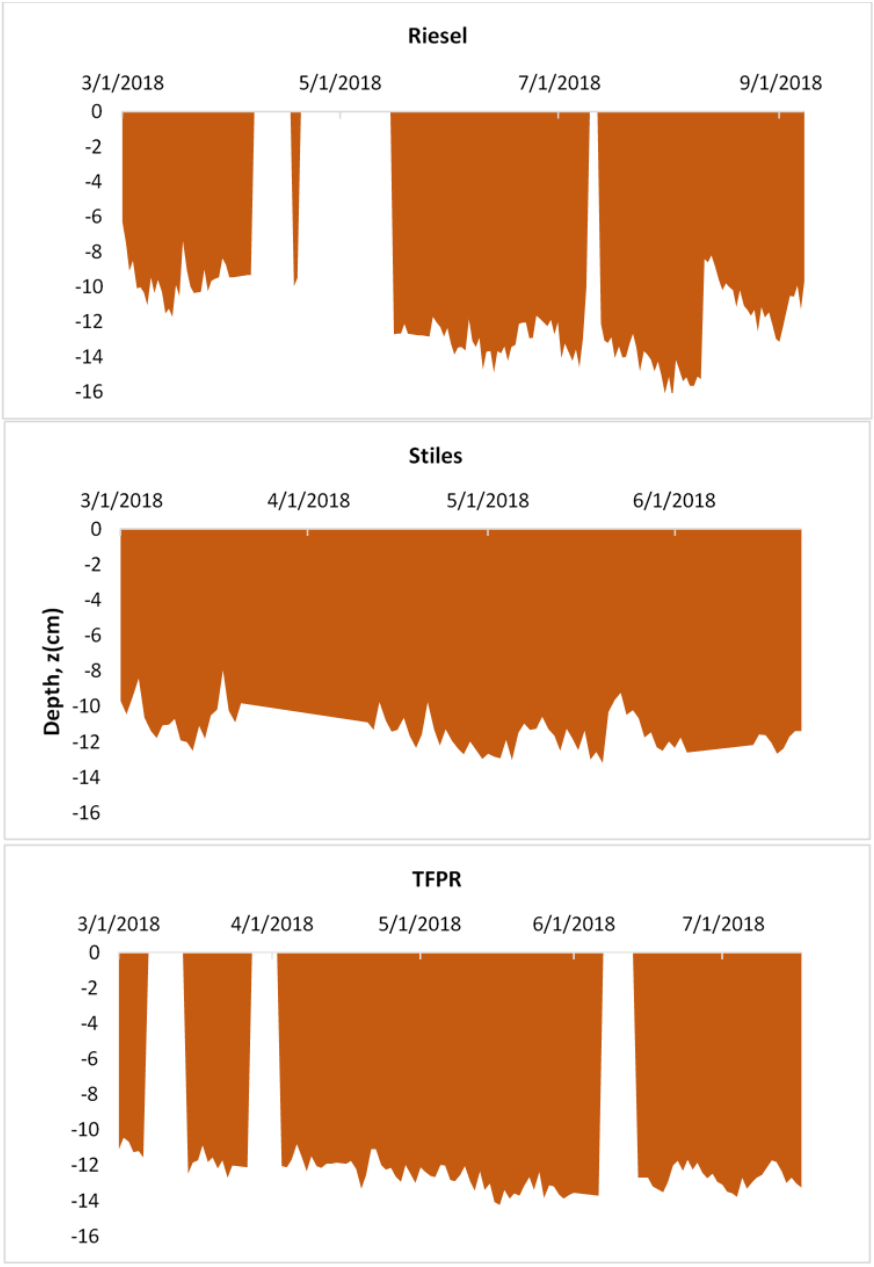

Figure 11 Vertical support of CRNS at the three sites during the study period

As we can see from the Figure 12, even though the model was unable to capture the peak values, the calibrated sensors demonstrated higher variability in soil moisture estimation. The mean modeled soil moisture for the study period at Riesel is 0.47 m^3m^{-3}, Stiles is 0.42 $m^3m^{-3}$and TFPR is 0.34 m^3m^{-3}. The mean CRNS derived soil moisture (θ_{CRNS}) using the NDVI independent N_o(eq. 7) for Riesel is 0.44 m^3m^{-3},Stiles is 0.43 m^3m^{-3} and TFPR is 0.33 m^3m^{-3}. Mean θ_{CRNS} obtained using the NDVI dependent estimate of N_o for Riesel, Stiles and TFPR is 0.43 m^3m^{-3}, 0.4 m^3m^{-3} and 0.32 m^3m^{-3} respectively which is less than the θ_{CRNS} for all the sites when the NDVI is not considered. The difference in the values may be due to the additional signals from the vegetation water content that have not been considered during optimization of parameters without considering the NDVI changes.

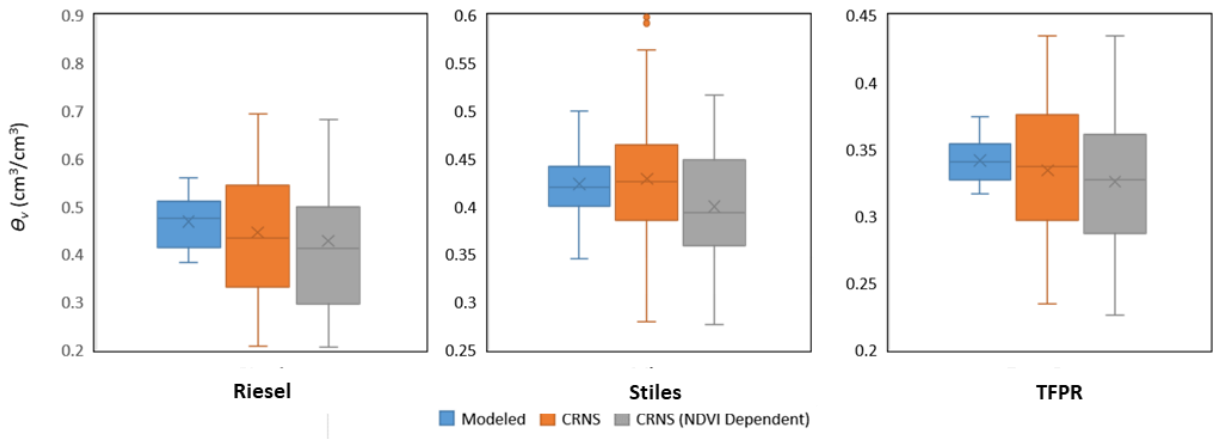

Figure 12 Comparison between Modeled Soil moisture, CRNS derived soil moisture using the regular raw neutron count (N_o) and CRNS derived soil moisture using NDVI dependent N_o

CHAPTER III

VALIDATION OF CALIBRATED CRNS USING GRAVIMETRIC SOIL MOISTURE AND EVAPOTRANSPIRATION ESTIMATES

In this chapter we discuss the validation of calibrated CRNS soil moisture products. Generally, gravimetric soil moisture calculated during different seasons is used for validation (Zreda et al., 2008; Hawdon et al., 2014). However, the process is particularly arduous in highly compacted clay soils. It is extremely, difficult to capture the complete range of soil moisture variation in these conditions. Therefore, exploiting the relationship between soil moisture and evapotranspiration (ET), we used ET products from eddy covariance towers and satellite measurements to validate our CNRS soil moisture products and cement the utility of our calibration procedure.

3.1 Validation using Gravimetric Soil Moisture Measurements

3.1.1 Field Campaigns

We measured the electrical conductivity of soil at Riesel and Stiles using an electromagnetic induction sensor, EM-38 (Fig. 13). The spatial distribution of electrical conductivity was assumed to correlate with the water holding capacity of the soil due to high clay content (Williams et al., 1987; Grisso et al., 2005). The location of the permanent soil moisture nodes (Table 1) were determined based on their spatial distribution. As there is only one soil node at the TFPR, electrical conductivity analysis was not performed.

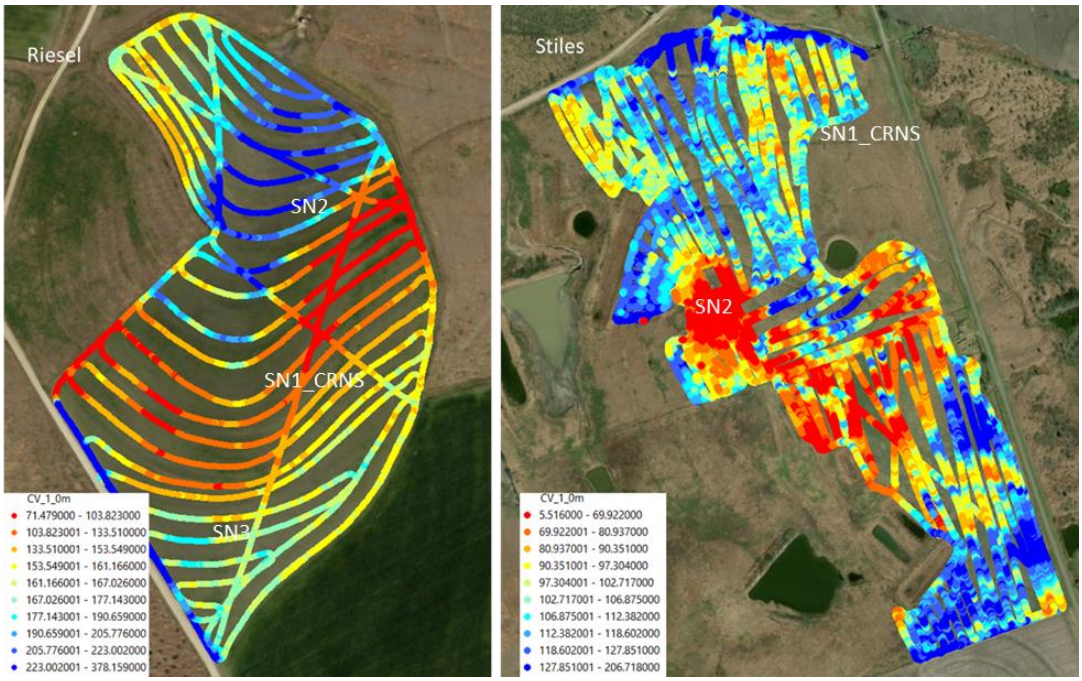

Figure 13 Electrical conductivity maps for (left) Riesel and (right) Stiles Farm for stratified sampling (TWO data repository). Higher conductance value corresponds to higher clay content in the soil

To determine gravimetric soil moisture at all the sites two field campaigns were conducted at each site. We performed stratified random sampling at depths of 5 cm, 10 cm, and 15 cm using the soil electrical conductivity map in Riesel and Stiles. We collected soil and vegetation samples at 8-10 locations during each visit. At TFPR we used radial sampling approach due to the absence of conductivity dataset. Therefore, we collected 14 samples at 3 depths each in 6 radial directions. The gravimetric soil moisture was obtained by oven drying for 2 days at a temperature of 110^{o}C.

3.2 Validation using ET from Satellite and Eddy Covariance Towers

3.2.1 Background

ET is a crucial component of the water cycle and the water budget equation. Quantification of ET is essential for irrigation water management, reservoir storage calculation, climate modeling, and disaster management. At field scale, better estimates are required to calculate crop water stress (Kirda et al., 2002, Rana et al., 1997). Agricultural drought monitoring is achieved using different ET based indices such as Evapotranspiration Deficit Index (ETDI) and Standardized Precipitation Evapotranspiration Index (SPEI) (Narsimhan et al., 2005; Vicente-Serrano et al., 2010). In urban areas where urban agriculture is gaining support, ET is used to determine the urban temperature changes (Qiu et al., 2013).

The precise measurement of ET is a challenge. Generally, reference crop ET is determined using the crop coefficient (K_c) (Kashyap et al., 2001; Djaman et al., 2012). But significant uncertainties have been observed in the ET estimates using K_c (Allen et al., 2005). Instruments such as Lysimeters and eddy covariance towers have been used to estimate the real-time actual ET. However, these instruments are expensive and their installation of posits a challenge. Indirect methods such as energy balance method, water budget method and empirical relationship between soil moisture and ET can produce reliable dataset (Xu et al., 2005; Allen et al. 2005; Allen et al. 2007).

Land surface models are used to determine ET by conserving energy or water balance by combining various meteorological and hydrological variables (Wang et al., 2012). Remote

sensing using thermal infrared (TIR) and visible-near infrared (VNIR) bands, and ground-based sensors can determine these variables at continuous timescales (Mu et al., 2007; Mu et al., 2011). Recently, energy-based Mapping ET at high Resolution with Internalized Calibration (METRIC) model which uses Landsat Thematic Mapper (TM) with weather station dataset can produce high-resolution estimates (Allen et al., 2007, Morton et al., 2013, Paco et al., 2014). Additionally, several algorithms have been developed using Moderate Resolution Spectroradiometer on Terra and Aqua (MODIS) satellites to prepare a repository of ET estimates at finer temporal resolution (Mu et al., 2007; Nagler et al., 2005;Mu et al., 2011).

To predict ET from soil moisture estimates, relationships have been developed between the two variables (Wetzel et al., 1987, Vivoni et al., 2008, Rodríguez-Iturbe et al., 2007). Soil moisture is relatively easier to monitor using point scale instruments and therefore, can be used to produce ET dataset at high temporal resolution.

3.2.2 METRIC Algorithm to Derive ET from Landsat-8 Thermal Sensors

METRIC algorithm uses Surface Energy Balance (SEBAL) and calibrates it using ground-based weather station dataset (Allen et al., 2007). The energy balance model SEBAL uses a near surface energy gradient (Bastiaanssen et al., 1995). ET can be calculated as the latent energy in the energy budget equation (eq. 9).

$$LE = R_n - G - H \tag{9}$$

Where LE = latent energy, R_n = net radiation, G = ground heat flux and H = sensible heat flux. METRIC prepares input for energy balance by combining ground based meteorological

dataset (wind speed, relative humidity, temperature and net incoming radiation), with satellite derived parameters (DEM, NDVI etc.).

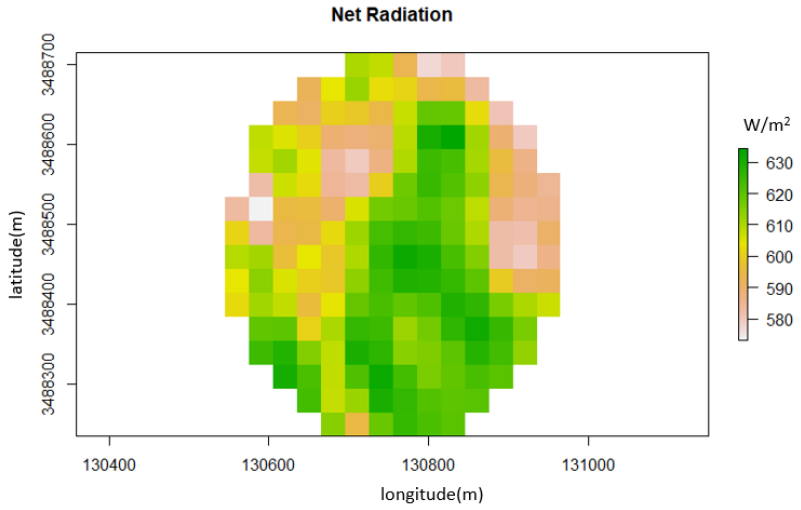

Figure 14 Net radiation Rn at Riesel on 7/21/18

3.2.2.1 Net Radiation

R_n (Fig. 14) is calculated by subtracting incoming radiation from the outgoing radiation (eq. 10).

$$R_n = RS_i - \alpha RS_i + RL_i - RL_o - (1 - \varepsilon_o)\, RL_i \quad (10)$$

Where RS and RL are shortwave and longwave radiation, where i and j denotes incoming and outgoing radiation. ε_o is surface emissivity and α is surface albedo (Fig. 15). The ground-based eddy covariance towers provide the incoming radiation data. Outgoing longwave

(11)

radiation is given by Stefan-Boltzman equation (eq. 11)

$$RL = \varepsilon_o \sigma T_s^4$$

T_s is surface temperature calculated using landsat images (Markham and Barker 1986) and σ is Stefan Boltzman constant (5.67 X 10^{-8} $Wm^{-2}K^{-4}$). Tasumi (2003) provides an empirical equation to determine ε_o by Leaf Area Index, LAI (Fig. 17) (eq. 12).

$$\varepsilon_o = \begin{cases} 0.95 + 0.01LAI, & LAI < 3 \\ 0.98 \quad , & LAI \geq 3 \end{cases} \quad (12)$$

Tasumi et al., (2007) provides calculation of surface albedo by integrating satellite reflectance from Landsat image with elevation from SRTM and humidity from the ground-based sensor (EWRI 2002).

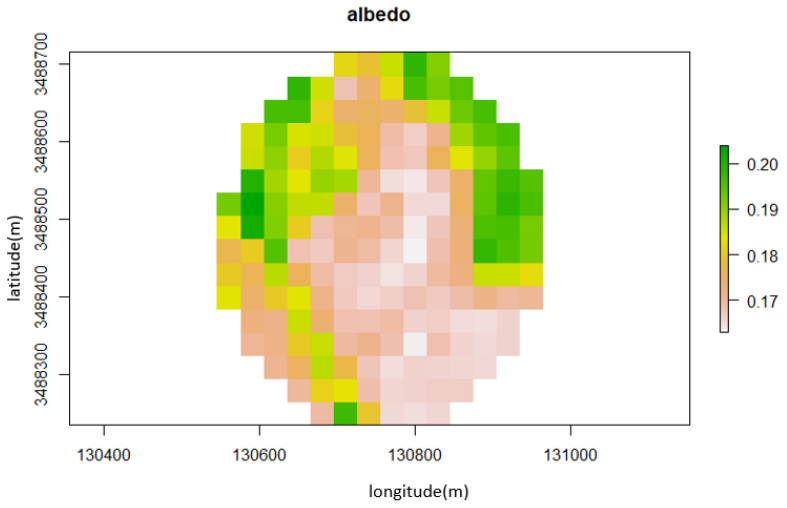

Figure 15 albedo, α at Riesel on 7/21/18

3.2.2.2 Ground Heat Flux

Bastiaanssen et al., (2000) developed an empirical equation to determine Ground heat flux, G (Fig. 16) using previously calculated R_n, T_s, α and Landsat based NDVI (eq. 13).

$$G = T_s\,(0.0038 + 0.0074\alpha)(1 - 0.98NDVI^4)R_n \quad (13)$$

NDVI is calculated using Landsat Near Infra-Red (NIR) and Red Bands. It is a measure of greenness of plants which can be used as a proxy for vegetation cover (eq. 14).

$$NDVI = \frac{NIR - Red}{NIR + Red} \quad (14)$$

In Landsat 8, Band 4 and Band 3 corresponds to NIR and Red bands respectively.

3.2.2.3 Sensible Heat Flux

One-dimensional aerodynamic function is used to calculate sensible heat flux(H) (Tasumi et al., 2005) (eq. 15)

$$H = \frac{\rho_{air} c_p (a + bT_s)}{r_{ah}} \quad (15)$$

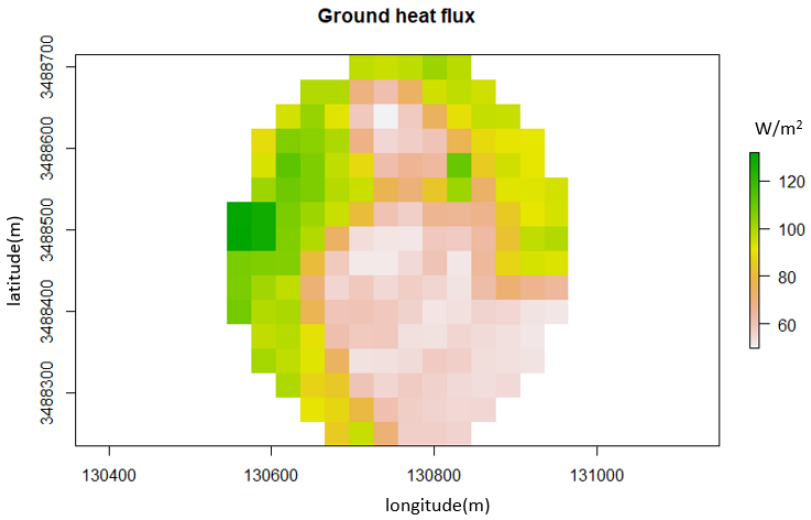

Figure 16 Ground heat flux, G at Riesel on 7/21/18

Where ρ_{air} is air density, c_p is the specific heat capacity (1004 $Jkg^{-1}K^{-1}$) and r_{ah} is aerodynamic resistance to heat transport. a and b are image based empirical coefficients that can be calculated using hot and cold pixels where temperature difference is calculated using CIMEC (Calibration using Inverse Modeling at Extreme Conditions) procedure (Allen et al., 2011). The cold pixel has high vegetation cover and hot pixels are the ones with dry bare soil. r_{ah} is a function of surface roughness, wind speed and vegetation height. We iteratively found the optimum no. of hot and cold pixels and (Bastiaanssen et al., 2000) which are then used to determine the sensible heat.

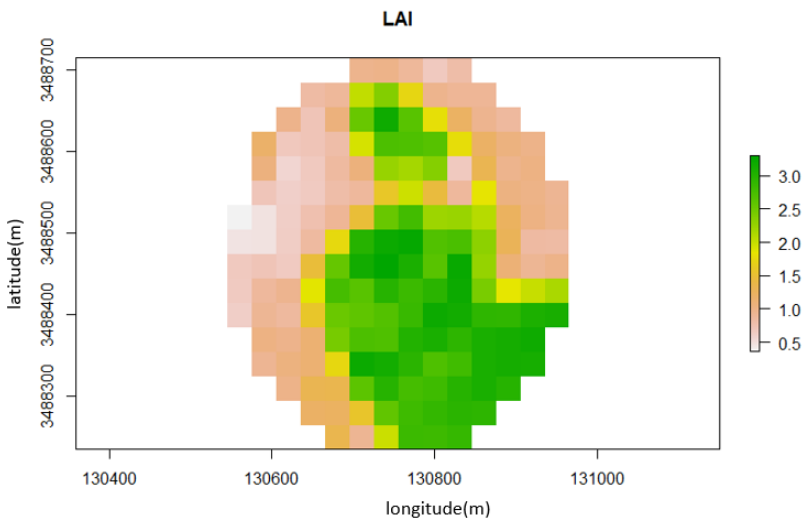

Figure 17 Leaf Area Index, LAI at Riesel on 7/21/18

We compute LE using R_n, H and G using equation 1. The ET is calculated in mm/day at the satellite overpass by dividing the LE value by latent heat of vaporization (λ). For illustration purpose Figure 14, 15, 16, and 17 shows the calculation for Riesel during the satellite overpass on 21stJuly 2018.

3.2.3 ET Derived from CRNS Measurements

Rodriguez – Iturbe et al., (2007) developed a piecewise linear relationship between soil moisture and ET (eq. 17).

$$ET(\theta) = \begin{cases} 0 & 0 < \theta \leq \theta_h \\ E_w \dfrac{\theta - \theta_h}{\theta_w - \theta_h} & \theta_h < \theta \leq \theta_w \\ E_w + (ET_{max} - E_w)\dfrac{\theta - \theta_h}{\theta^* - \theta_w} & \theta_w < \theta \leq \theta^* \\ ET_{max} & \theta^* < \theta \leq \theta_p \end{cases} \quad (16)$$

Where θ_h , θ_w, and θ^* are hygroscopic, wilting point and plant water stress inflection point for respectively, E_w is soil evaporation, ET_{max} is maximum ET and $\theta_p$is pore water capacity of the soil which was assumed to be equal to saturated water content $\theta_s$obtained from inverse modelling calculations.We optimized the parameters in eq. 15 using SCE-UA (Duan et al., 1993). We minimized the RMSE between observed ET from Eddy covariance and simulated values (eq. 16).We ran the simulation on daily timestep for better computational efficiency. Although, SCE-UA is a single objective optimization algorithm, we gathered the variance of the simulated values, after each evolution cycle to make an informed decision regarding the parameters. The time period of simulation was set according to the availability of eddy covariance and CRNS dataset.

3.3 Results

3.3.1 Validation using In-Situ Gravimetric Samples

We performed validation for Riesel on two days in the month of March and July while collecting and analyzing at least 8 samples during each visit. The RMSE between CRNS soil moisture (θ_{CRNS}) and water content of the oven dried soil (θ_d) is 0.04 approximately. At Stiles we collected the 6 samples in March and July each. The RMSE of validation for stiles is 0.035m^3m^{-3}. We collected 14 samples in TFPR in April (Fig. 23) and June each and found the RMSE to be approximately 0.04m^3m^{-3}. The value of soil moisture is overestimated by the CRNS in all cases. Results indicate the importance of including vegetation water content (here NDVI) in the model-based approach where calibration is performed on a continuous timescale.

Figure 18 The gravimetric soil samples being prepared for oven drying at 110 ^{o}C

3.3.2 Validation using Satellite and Eddy Covariance based ET

3.3.2.1 Calculation of Landsat based ET using METRIC algorithm

Figure 19 illustrates the METRIC-ET in Riesel, TFPR and Stiles farm. The spatially averaged ET at Riesel, TFPR and Stiles farm was compared against the ET from Eddy Covariance towers present at the three sites. The RMSE at Riesel, Stiles and TFPR is 2.67 mm/day, 2.36 mm/day and 2.6 mm/day respectively (Table5). The values are slightly higher than the previous studies which were conducted in different hydroclimates (Numata et al., 2007; Wagle et al., 2017). The highest values ET were calculated during the summer months when the temperature is highest at the three sites.

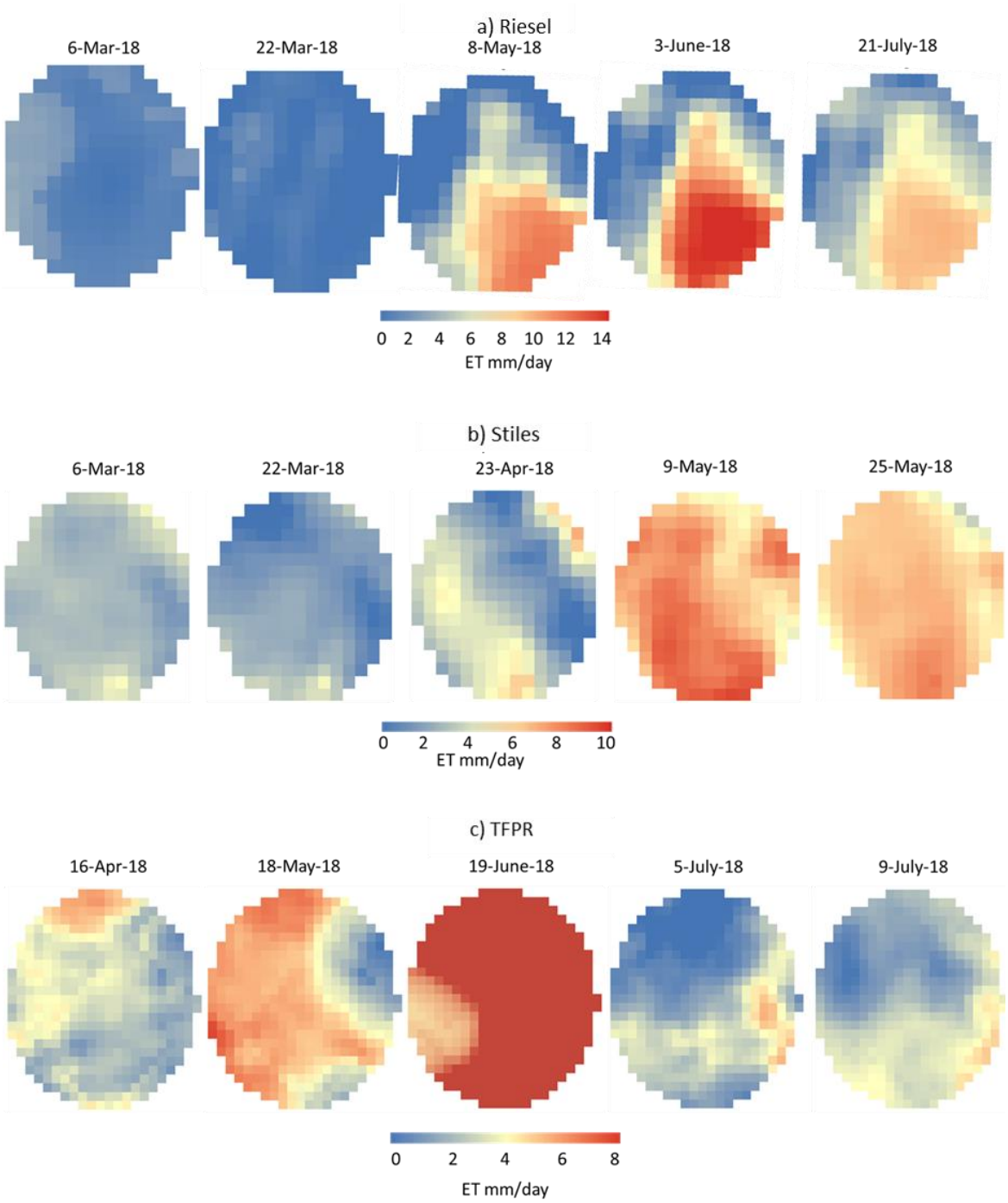

Figure 19 Landsat 8 ET estimates derived using METRIC algorithm at a) Riesel, b) Stiles, and c) TFPR

METRIC performed well during the spring and autumn season. The algorithm overestimated the values during summer months of May, June and July at all sites (Fig. 20). We observed low values of ET (0.31 mm/day on 6 March in Riesel, 0.4 mm/day on 19 June in TFPR) on some days, which may be have occurred due to the cloudy conditions during the satellite overpass. The accuracy of the model is subjected to the performance of meteorological sensors present at the site.

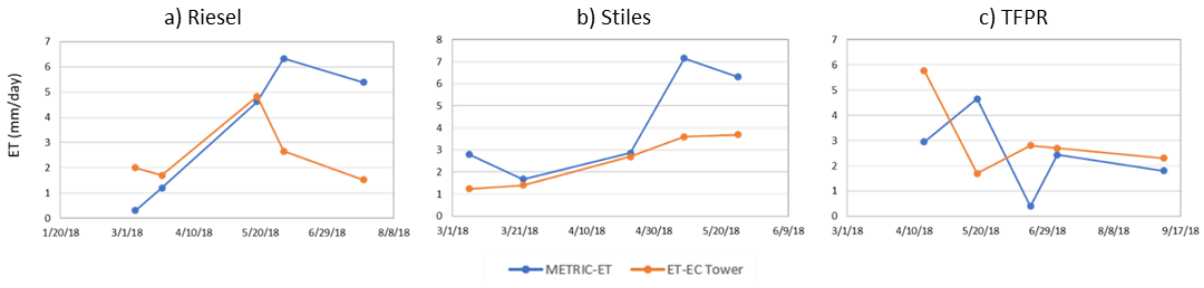

Figure 20 Comparison between METRIC-ET and ET from eddy covariance towers at a) Riesel, b) Stiles, c) TFPR

3.3.2.2 Comparison between CRNS-ET and METRIC ET

Table 5 shows the optimized regression parameters used in the validation studies. Due to the soil texture the values were higher than expected. RMSE between the observed and simulated values at Riesel, Stiles and TFPR are slightly higher than in the previous studies (Vivoni et al., 2008; Schreiner-McGraw et al., 2016). Comparatively, Stiles had the lowest overall ET, consistent with low θ_{CRNS} values at the site. It must be noted that the values are only to validate the performance of the sensors as the regression model is developed for point scale dataset (Rodriguez-Iturbe et al2007). Figure 21 illustrates the comparison between the three ET

estimates. The CRNS-ET replicated EC-ET better than the METRIC-ET. In figure 21 we see fewer values of METRIC ET in Stiles and TFPR due to limited availability of corrected CRNS dataset. But we compared the complete METRIC-ET and CRNS-ET dataset (Table 6) irrespective of time period to test the efficacy of CRNS using ET as a proxy.

Table 5 Regression Parameters for nonlinear piecewise relationship between θ_{CRNS} and ET from eddy covariance stations at the three sites

Site	θ_h m^3m^{-3}	θ_w m^3m^{-3}	θ^* m^3m^{-3}	E_w mm/day	ET_{max} mm/day	RMSE mm/day
Riesel	0.18	0.27	0.51	0.23	3.31	1.31
Stiles	0.17	0.34	0.59	0.16	3.20	1.38
TFPR	0.05	0.23	0.52	2.88	5.80	1.51

Table 6 shows the comparison between CRNS-ET and METRIC ET. We observe a reduction of 30-50% in RMSE at all three sites cementing the utility of CRNS for improving the estimates. Therefore, the performance of CRNS-ET at all three sites is better than the METRIC-ET. The better estimates prove the validity of our model-based calibration approach for CRNS.

Table 6 Comparison between CRNS-ET and METRIC-ET

Site	METRIC-ET RMSE mm/day	CRNS-ET RMSE mm/day	Improvement %
Riesel	2.51	1.31	47
Stiles	2.10	1.38	34
TFPR	2.13	1.51	30

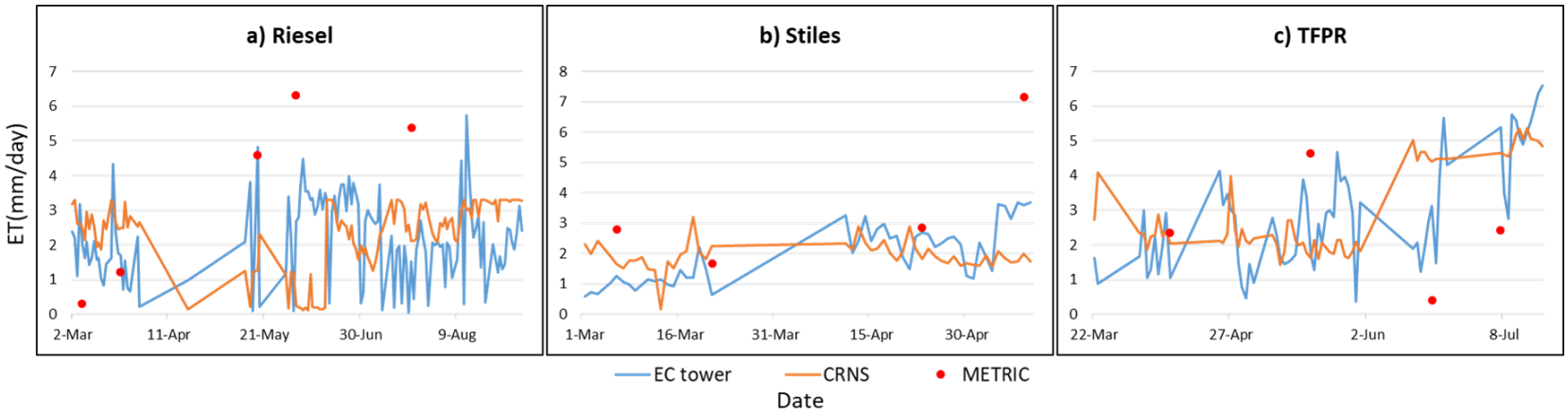

Figure 21 ET at a) Riesel, b) Stiles and c) TFPR from EC Towers, derived from CRNS using piecewise linear regression and Landsat using METRIC algorithm

CHAPTER IV

SUMMARY AND CONCLUSION

In this study, we calibrated the CRNS for mixed land use/landcover in Lower Brazos River Basin by numerical simulation of soil moisture dynamics in Hydrus 2D framework. We used SCE-UA to optimize vegetation based effective soil hydraulic parameters by minimizing the difference between numerically simulated and observed soil moisture from the soil moisture probes at the site. We calculated vegetation-based calibration parameter N_o to determine θ_{CRNS}. We observed a higher variability in θ_{CRNS} compared to the θ_{Model}. Thus, the complete distribution of soil moisture in the study period was captured by CRNS. We validated the values making use of a state variable, θ and atmospheric forcing, ET. We compared θ_{CRNS} with in-situ soil moisture from various field campaigns and found satisfactory results. We derived ET, CRNS estimates using piecewise linear regression (eq. 16) and validated it against the ET estimates from Landsat 8 gathered by using METRIC algorithm. The CRNS improved the results considerably proving the utility of our calibration approach. Traditional validation using gravimetric soil moisture performed well in TFPR (Managed Prairie) and Stiles (Traditional Prairie) with RMSE ranging from $0.039 m^3m^{-3}$-$0.044\ m^3m^{-3}$. The method did not produce satisfactory results at Riesel (Traditional Agriculture) further necessitating the study on the effects of vegetation on the CRNS signals.

In addition to that, we calculated the time series of the penetration depth of the CRNS using which can serve as a platform for future calibration studies on similar soils and land

use/land cover types. We were able to achieve our objective to cut short the laborious process involved in the in-situ calibration of CRNS.

In Texas, recent prolonged drought periods have compelled farmers to switch to sensor driven agriculture (Weiser 2015). Real time estimation of soil moisture is an important part of this change. However, poor performance of the in-situ soil moisture sensors in soils with high clay content can be a challenge contributing towards bad farm practices. Satellite estimates have a coarse resolution and continuous estimation is a challenge. Therefore, CRNS presents itself as a novel method to non-invasively determine soil moisture at a farm support scale. Model based and vegetation dependent calibration approach has proven that its usefulness in providing good observations. We have shown, even if our model is not up to the mark, if we can make an educated guess regarding the calibration parameters, we can achieve reliable estimates of soil moisture from the sensors. But there is still, a lot of room for improvement. The vegetation water content which contributes significantly towards the signal should be characterized and removed for better performance of CRNS.

REFERENCES

Albergel, C., De Rosnay, P., Gruhier, C., Muñoz-Sabater, J., Hasenauer, S., et al. "Evaluation of remotely sensed and modeled soil moisture products using global ground-based in situ observations." *Remote Sensing of Environment* 118 (2012): 215-226.

Allen, R.G., Tasumi, M. and Trezza, R. "Satellite-based energy balance for mapping evapotranspiration with internalized calibration (METRIC)—Model." *Journal of irrigation and drainage engineering* 133.4 (2007): 380-394.

Allen, R., Irmak, A., Trezza, R., Hendrickx, J.M.H., Bastiaanssen, W., Kjaersgaard, J. Satellite-based ET estimation in agriculture using SEBAL and METRIC. *Hydrol. Process.*25 (2011): 4011–4027

Alley, William M. "The Palmer drought severity index: limitations and assumptions." *Journal of climate and applied meteorology* 23.7 (1984): 1100-1109.

Avery, W.A., Finkenbiner, C., Franz, T.E., Wang, T., Nguy-Robertson, A.L., et al. "Incorporation of globally available datasets into the roving cosmic-ray neutron probe method for estimating field-scale soil water content." *Geophysical Research Letters* (2016): doi.org/10.1002/grl.50791

Baatz, R., Bogena, H.R., Hendricks Franssen, H.J., Huisman, J.A., Montzka, C. and Vereecken, H. "An empirical vegetation correction for soil water content quantification using cosmic ray probes." *Water Resources Research* 51.4 (2015): 2030-2046.

Bastiaanssen, W.G., Menenti, M., Feddes, R.A. and Holtslag, A.A.M. "A remote sensing surface energy balance algorithm for land (SEBAL). 1. Formulation." *Journal of hydrology* 212 (1998): 198-212.

Bastiaanssen, Wim GM. "SEBAL-based sensible and latent heat fluxes in the irrigated Gediz Basin, Turkey." *Journal of hydrology* 229.1-2 (2000): 87-100.

Baroni, G., Scheiffele, L.M., Schrön, M., Ingwersen, J. and Oswald, S.E. "Uncertainty, sensitivity and improvements in soil moisture estimation with cosmic-ray neutron sensing." *Journal of hydrology* 564 (2018): 873-887.

Bogena, H.R., Huisman, J.A., Baatz, R., Hendricks Franssen, H.J. and Vereecken, H. "Accuracy of the cosmic-ray soil water content probe in humid forest ecosystems: The worst case scenario." *Water Resources Research* 49.9 (2013): 5778-5791.

Brocca, L., Melone, F., Moramarco, T., Wagner, W., Naeimi, V., et al. "Improving runoff prediction through the assimilation of the ASCAT soil moisture product." *Hydrology and Earth System Sciences* 14.10 (2010): 1881-1893.

Cai, X., McKinney, D.C. and Lasdon, L.S. "Integrated hydrologic-agronomic-economic model for river basin management." *Journal of water resources planning and management* 129.1 (2003): 4-17.

Campbell, G.S. and Campbell, M.D. "Irrigation scheduling using soil moisture measurements: theory and practice." *Advances in irrigation* 1 (1982): 25-42.

Chen, M., Willgoose, G.R. and Saco, P.M. "Spatial prediction of temporal soil moisture dynamics using Hydrus-1D." *Hydrological Processes* 28.2 (2014): 171-185.

Coopersmith, E.J., Cosh, M.H. and Daughtry, C.S. "Field-scale moisture estimates using CRNS sensors: A validation study with temporary networks and leaf-area-indices." *Journal of hydrology* 519 (2014): 637-643.

Cosh, M.H., Jackson, T.J., Bindlish, R. and Prueger, J.H. "Watershed scale temporal and spatial stability of soil moisture and its role in validating satellite estimates." *Remote sensing of Environment* 92.4 (2004): 427-435.

Cosh, M.H., Jackson, T.J., Starks, P. and Heathman, G. "Temporal stability of surface soil moisture in the Little Washita River watershed and its applications in satellite soil moisture product validation." *Journal of Hydrology* 323.1-4 (2006): 168-177.

Crow, W.T. and Wood, E.F. "The assimilation of remotely sensed soil brightness temperature imagery into a land surface model using ensemble Kalman filtering: A case study based on ESTAR measurements during SGP97." *Advances in Water Resources* 26.2 (2003): 137-149.

Dai, A., Trenberth, K.E. and Qian, T. "A global dataset of Palmer Drought Severity Index for 1870–2002: Relationship with soil moisture and effects of surface warming." *Journal of Hydrometeorology* 5.6 (2004): 1117-1130

Datta, S., Taghvaeian, S., Ochsner, T., Moriasi, D., Gowda, P. and Steiner, J. "Performance Assessment of Five Different Soil Moisture Sensors under Irrigated Field Conditions in Oklahoma." *Sensors* 18.11 (2018): 3786.

Desilets, D., Zreda, M. and Ferré, T.P. "Nature's neutron probe: Land surface hydrology at an elusive scale with cosmic rays." *Water Resources Research* 46.11 (2010): doi.org/10.1029/2009WR008726

Djaman, K. and Irmak, S. "Actual crop evapotranspiration and alfalfa-and grass-reference crop coefficients of maize under full and limited irrigation and rainfed conditions." *Journal of Irrigation and Drainage Engineering* 139.6 (2012): 433-446.

Duan, Q.Y., Gupta, V.K. and Sorooshian, S. "Shuffled complex evolution approach for effective and efficient global minimization." *Journal of optimization theory and applications* 76.3 (1993): 501-521.

Durner, W., Jansen, U. and Iden, S.C. "Effective hydraulic properties of layered soils at the lysimeter scale determined by inverse modelling." *European Journal of Soil Science* 59.1 (2008): 114-124.

Feddes, R.A., Bresler, E. and Neuman, S.P."Field test of a modified numerical model for water uptake by root systems." *Water Resources Research* 10.6 (1974): 1199-1206.

Franz, T.E., Zreda, M., Rosolem, R. and Ferre, T.P.A "Field validation of a cosmic-ray neutron sensor using a distributed sensor network." *Vadose Zone Journal* 11.4 (2012): doi.org/10.2136/vzj2012.0046

Franz, T.E., Zreda, M., Rosolem, R. and Ferre, T.P.A. "A universal calibration function for determination of soil moisture with cosmic-ray neutrons." *Hydrology and Earth System Sciences* 17.2 (2013): 453-460.

Grisso, R.D., Alley, M.M., Holshouser, D.L. and Thomason, W.E. "Precision Farming Tools: Soil Electrical Conductivity." Virginia Cooperative Extension (2005): 442-508

Guo, J., Zhou, J., Zou, Q., Liu, Y. and Song, L. "A novel multi-objective shuffled complex differential evolution algorithm with application to hydrological model parameter optimization." *Water resources management* 27.8 (2013): 2923-2946.

Hawdon, A., McJannet, D. and Wallace, J. "Calibration and correction procedures for cosmic-ray neutron soil moisture probes located across Australia." *Water Resources Research* 50.6 (2014): 5029-5043.

Henderson-Sellers, A., Yang, Z.L. and Dickinson, R.E. "The project for intercomparison of land-surface parameterization schemes." *Bulletin of the American Meteorological Society*74.7 (1993): 1335-1350.

Hoekstra, A.Y., Mekonnen, M.M., Chapagain, A.K., Mathews, R.E. and Richter, B.D. "Global monthly water scarcity: blue water footprints versus blue water availability." *PLoS One* 7.2 (2012): e32688.

Huisman, J.A., Sperl, C., Bouten, W. and Verstraten, J.M. "Soil water content measurements at different scales: accuracy of time domain reflectometry and ground-penetrating radar." Journal of Hydrology 245.1-4 (2001): 48-58.

Jacobs, J.M., Mohanty, B.P., Hsu, E.C., and Miller , D.A. "SMEX02: Field scale variability, time stability and similarity of soil moisture." *Remote sensing of Environment* 92.4 (2004): 436-446.

Jetten, V., De Roo, A.D. and Favis-Mortlock, D. "Evaluation of field-scale and catchment-scale soil erosion models." *Catena* 37.3-4 (1999): 521-541.

Jia, Z., Liu, S.M., Xu, W., Chen, Y. and Zhu, M., "Validation of remotely sensed evapotranspiration over the Hai River Basin, China." *Journal of Geophysical Research: Atmospheres* 117.D13 (2012): doi.org/10.1029/2011JD017037

Joshi, C., and Mohanty, B.P. "Physical controls of near-surface soil moisture across varying spatial scales in an agricultural landscape during SMEX02." *Water Resources Research* 46.12 (2010): doi.org/10.1029/2010WR009152

Kashyap, P. S., and Panda, R.K. "Evaluation of evapotranspiration estimation methods and development of crop-coefficients for potato crop in a sub-humid region." *Agricultural water management* 50.1 (2001): 9-25.

Kirda, C. "Deficit irrigation scheduling based on plant growth stages showing water stress tolerance." *Deficit irrigation practices* (2002): 3-10

Kirkby, M.J., Imeson, A.C., Bergkamp, G. and Cammeraat, L.H. "Scaling up processes and models from the field plot to the watershed and regional areas." *Journal of Soil and Water Conservation* 51.5 (1996): 391-396.

Kool, D., Agam, N., Lazarovitch, N., Heitman, J.L., Sauer, T.J. and Ben-Gal, A. "A review of approaches for evapotranspiration partitioning." *Agricultural and forest meteorology* 184 (2014): 56-70.

Koster, R.D., Guo, Z., Yang, R., Dirmeyer, P.A., Mitchell, K. and Puma, M.J. "On the nature of soil moisture in land surface models." *Journal of Climate* 22.16 (2009): 4322-4335.

Leib, B.G., Jabro, J.D. and Matthews, G.R. "Field evaluation and performance comparison of soil moisture sensors." *Soil Science* 168.6 (2003): 396-408.

Lorenz, R., Jaeger, E.B. and Seneviratne, S.I. "Persistence of heat waves and its link to soil moisture memory." *Geophysical Research Letters* 37.9 (2010): doi.org/10.1029/2010GL042764

Lv, L., Franz, T.E., Robinson, D.A. and Jones, S.B. "Measured and modeled soil moisture compared with cosmic-ray neutron probe estimates in a mixed forest." *Vadose Zone Journal* 13.12 (2014): doi.org/10.2136/vzj2014.06.0077

Markham, B. L. "Landsat MSS and TM post-calibration dynamic ranges, exoatmospheric reflectances and at-satellite temperatures." *Landsat Technical Notes 1* (1986): 3-8

Martínez-Fernández, J. , and Ceballos, A. "Temporal stability of soil moisture in a large-field experiment in Spain." *Soil Science Society of America Journal* 67.6 (2003): 1647-1656.

Matgen, P., Heitz, S., Hasenauer, S., Hissler, C., Brocca, L., Hoffmann, L., et al. "On the potential of MetOp ASCAT-derived soil wetness indices as a new aperture for hydrological monitoring and prediction: a field evaluation over Luxembourg." *Hydrological Processes* 26.15 (2012): 2346-2359.

Malbéteau, Y., Merlin, O., Molero, B., Rüdiger, C. and Bacon, S. "DisPATCh as a tool to evaluate coarse-scale remotely sensed soil moisture using localized in situ measurements: Application to

SMOS and AMSR-E data in Southeastern Australia." *International journal of applied earth observation and geoinformation* 45 (2016): 221-234.

McCabe, M.F., Gao, H. and Wood, E.F. "Evaluation of AMSR-E-derived soil moisture retrievals using ground-based and PSR airborne data during SMEX02." Journal of Hydrometeorology 6.6 (2005): 864-877.

Merlin, O., Walker, J.P., Chehbouni, A. and Kerr, Y. "Towards deterministic downscaling of SMOS soil moisture using MODIS derived soil evaporative efficiency." *Remote Sensing of Environment* 112.10 (2008): 3935-3946.

Mittelbach, H., Lehner, I. and Seneviratne, S.I. "Comparison of four soil moisture sensor types under field conditions in Switzerland." Journal of Hydrology 430 (2012): 39-49.

Mohanty, B.P., and Mousli, Z. "Saturated hydraulic conductivity and soil water retention properties across a soil-slope transition." *Water Resources Research* 36.11 (2000): 3311-3324.

Mohanty, Binayak P., et al., "Field Sites." *Texas Water Observatory* (2015): two.tamu.edu/sites.aspx.

Mohanty, B.P., Cosh, M.H., Lakshmi, V. and Montzka, C. "Soil moisture remote sensing: State-of-the-science." *Vadose Zone Journal* 16.1 (2017): doi.org/10.2136/vzj2016.10.0105

Montzka, C., Bogena, H.R., Weihermuller, L., Jonard, F., Bouzinac, C., et al. "Brightness temperature and soil moisture validation at different scales during the SMOS validation campaign in the Rur and Erft catchments, Germany." *IEEE Transactions on Geoscience and Remote Sensing* 51.3 (2012): 1728-1743.

Morton, C.G., Huntington, J.L., Pohll, G.M., Allen, R.G., McGwire, K.C. and Bassett, S.D. "Assessing calibration uncertainty and automation for estimating evapotranspiration from agricultural areas using METRIC." *JAWRA Journal of the American Water Resources Association* 49.3 (2013): 549-562.

Mu, Q., Heinsch, F.A., Zhao, M. and Running, S.W. "Development of a global evapotranspiration algorithm based on MODIS and global meteorology data." *Remote sensing of Environment* 111.4 (2007): 519-536.

Mu, Q., Zhao, M. and Running, S.W. "Improvements to a MODIS global terrestrial evapotranspiration algorithm." *Remote Sensing of Environment* 115.8 (2011): 1781-1800.

Münier, B., Birr-Pedersen, K. and Schou, J.S. "Combined ecological and economic modelling in agricultural land use scenarios." *Ecological Modelling* 174.1-2 (2004): 5-18.

Muñoz-Carpena, R. and Dukes, M.D. "Automatic irrigation based on soil moisture for vegetable crops." , Institute of Food and Agricultural Sciences, Univ. of Florida, Gainesville, Florida, *Nutrient Management of Vegetable and Row Crops Handbook* 173 (2015).

Nagler, P.L., Scott, R.L., Westenburg, C., Cleverly, J.R., Glenn, E.P. and Huete, A.R. "Evapotranspiration on western US rivers estimated using the Enhanced Vegetation Index from MODIS and data from eddy covariance and Bowen ratio flux towers." *Remote sensing of environment* 97.3 (2005): 337-351.

Narasimhan, B., and Srinivasan, R. "Development and evaluation of Soil Moisture Deficit Index (SMDI) and Evapotranspiration Deficit Index (ETDI) for agricultural drought monitoring." *Agricultural and Forest Meteorology* 133.1-4 (2005): 69-88.

Narayan, U., Lakshmi, V. and Jackson, T.J. "High-resolution change estimation of soil moisture using L-band radiometer and radar observations made during the SMEX02 experiments." *IEEE Transactions on Geoscience and Remote Sensing* 44.6 (2006): 1545-1554.

Njoku, E.G., Wilson, W.J., Yueh, S.H., Dinardo, S.J., Li, F.K. and Jackson, T.J. "Observations of soil moisture using a passive and active low-frequency microwave airborne sensor during SGP99." *IEEE Transactions on Geoscience and Remote Sensing* 40.12 (2002): 2659-2673.

Das, N. N., and Mohanty, B.P. "Root zone soil moisture assessment using remote sensing and vadose zone modeling." *Vadose Zone Journal* 5.1 (2006): 296-307.

Paço, T.A., Pôças, I., Cunha, M., Silvestre, J.C., Santos, F.L., Paredes, P. and Pereira, L.S. "Evapotranspiration and crop coefficients for a super intensive olive orchard. An application of SIMDualKc and METRIC models using ground and satellite observations." *Journal of hydrology* 519 (2014): 2067-2080.

Qiu, G.Y., LI, H.Y., Zhang, Q.T., Wan, C.H.E.N., Liang, X.J. and Li, X.Z. "Effects of evapotranspiration on mitigation of urban temperature by vegetation and urban agriculture." *Journal of Integrative Agriculture* 12.8 (2013): 1307-1315.

Rana, G., Katerji, N. and de Lorenzi, F. "Measurement and modelling of evapotranspiration of irrigated citrus orchard under Mediterranean conditions." *Agricultural and Forest Meteorology* 128.3-4 (2005): 199-209.

Ragab, R., Evans, J.G., Battilani, A. and Solimando, D. "The cosmic-ray soil moisture observation system (CRNS) for estimating the crop water requirement: new approach." *Irrigation and drainage* 66.4 (2017): 456-468.

Reynolds, W. D., E. G. Gregorich, and W. E. Curnoe. "Characterisation of water transmission properties in tilled and untilled soils using tension infiltrometers." *Soil and Tillage Research* 33.2 (1995): 117-131.

Rodell, M., Velicogna, I. and Famiglietti, J.S. "Satellite-based estimates of groundwater depletion in India." *Nature* 460.7258 (2009): 999.

Rodríguez-Iturbe, I. and Porporato, A. “Ecohydrology of water-controlled ecosystems: soil moisture and plant dynamics”. *Cambridge University Press*, 2007.

Rosolem, R., Shuttleworth, W.J., Zreda, M., Franz, T.E., Zeng, X. and Kurc, S.A. "The effect of atmospheric water vapor on neutron count in the cosmic-ray soil moisture observing system." *Journal of Hydrometeorology* 14.5 (2013): 1659-1671.

Saadi, S., Boulet, G., Bahir, M., Brut, A., Delogu, É., Fanise, P., Mougenot, B. "Assessment of actual evapotranspiration over a semiarid heterogeneous land surface by means of coupled low-resolution remote sensing data with an energy balance model: comparison to extra-large

aperture scintillometer measurements." *Hydrology and Earth System Sciences* 22.4 (2018): 2187-2209.

Shea, M.A. and Smart, D.F. "Vertical cutoff rigidities for cosmic ray stations since 1955." *International Cosmic Ray Conference*. Vol. 10 (2001): 4063

Schaap, M.G., Leij, F.J. and Van Genuchten, M.T. "Rosetta: A computer program for estimating soil hydraulic parameters with hierarchical pedotransfer functions." *Journal of hydrology* 251.3-4 (2001): 163-176.

Schreiner-McGraw, A.P., Vivoni, E.R., Mascaro, G. and Franz, T.E. "Closing the water balance with cosmic-ray soil moisture measurements and assessing their relation to evapotranspiration in two semiarid watersheds." *Hydrology and earth system sciences* 20.1 (2016): 329.

Simpson, John A. "The cosmic ray nucleonic component: The invention and scientific uses of the neutron monitor." *Cosmic Rays and Earth*. Springer, Dordrecht, (2000): 11-32.

Simunek, J. and Van Genuchten, M.T. "Using the Hydrus-1D and Hydrus-2D codes for estimating unsaturated soil hydraulic and solute transport parameters." *Characterization and measurement of the hydraulic properties of unsaturated porous media* 1 (1999): 523-1.

Sorooshian, S., Duan, Q. and Gupta, V.K. "Calibration of rainfall-runoff models: Application of global optimization to the Sacramento Soil Moisture Accounting Model." *Water resources research* 29.4 (1993): 1185-1194.

Stéfanon, M., Drobinski, P., D'Andrea, F., Lebeaupin-Brossier, C. and Bastin, S. "Soil moisture-temperature feedbacks at meso-scale during summer heat waves over Western Europe." *Climate dynamics* 42.5-6 (2014): 1309-1324.

Tasumi, M., Trezza, R., Allen, R.G. and Wright, J.L. "Operational aspects of satellite-based energy balance models for irrigated crops in the semi-arid US." *Irrigation and Drainage Systems* 19.3-4 (2005): 355-376.

Tasumi, M. and Allen, R.G. "Satellite-based ET mapping to assess variation in ET with timing of crop development." *Agricultural Water Management* 88.1-3 (2007): 54-62.

Tian, Z., Li, Z., Liu, G., Li, B. and Ren, T. "Soil water content determination with cosmic-ray neutron sensor: Correcting aboveground hydrogen effects with thermal/fast neutron ratio." *Journal of Hydrology*540 (2016): 923-933.

Van Dam, J.C., Huygen, J., Wesseling, J.G., Feddes, R.A., Kabat, P., et al. "Theory of SWAP version 2.0; Simulation of water flow, solute transport and plant growth in the soil-water-atmosphere-plant environment.", *Technical Document 45,* No. 71. DLO Winand Staring Centre, (1997).

Van Genuchten, M. Th, and Nielsen, D.R. "On describing and predicting the hydraulic properties." *Annales Geophysicae*. Vol. 3. No. 5. (1985): 615-628

Vellidis, G., Tucker, M., Perry, C., Kvien, C. and Bednarz, C. "A real-time wireless smart sensor array for scheduling irrigation." *Computers and electronics in agriculture* 61.1 (2008): 44-50.

Vicente-Serrano, S.M., Beguería, S. and López-Moreno, J.I. "A multiscalar drought index sensitive to global warming: the standardized precipitation evapotranspiration index." *Journal of climate* 23.7 (2010): 1696-1718.

Vivoni, E.R., Moreno, H.A., Mascaro, G., Rodriguez, J.C., Watts, C.J., et al. "Observed relation between evapotranspiration and soil moisture in the North American monsoon region." *Geophysical Research Letters* 35.22 (2008): doi.org/10.1029/2008GL036001

Wang, C., Zuo, Q. and Zhang, R. "Estimating the necessary sampling size of surface soil moisture at different scales using a random combination method." *Journal of Hydrology* 352.3-4 (2008): 309-321.

Wang, K. and Dickinson, R.E. "A review of global terrestrial evapotranspiration: Observation, modeling, climatology, and climatic variability." *Reviews of Geophysics* 50.2 (2012).

Wang, J., Ge, Y., Heuvelink, G. and Zhou, C. "Upscaling in situ soil moisture observations to pixel averages with spatio-temporal geostatistics." *Remote Sensing* 7.9 (2015): 11372-11388.

Weiser, Matt. “Farm Sensors, Software and Growing More Food with Less Water.” *GreenBiz*, GreenBiz Group Inc., 12 Aug. 2015, *www.greenbiz.com/article/farm-sensors-software-and-growing-more-food-less-water*

Western, A.W., Zhou, S.L., Grayson, R.B., McMahon, T.A., Blöschl, G. and Wilson, D.J. "Spatial correlation of soil moisture in small catchments and its relationship to dominant spatial hydrological processes." *Journal of Hydrology* 286.1-4 (2004): 113-134.

Wetzel, P.J. and Chang, J.T. "Concerning the relationship between evapotranspiration and soil moisture." *Journal of climate and applied meteorology* 26.1 (1987): 18-27.

Williams, B.G. and Hoey, D. "The use of electromagnetic induction to detect the spatial variability of the salt and clay contents of soils." Soil Research 25.1 (1987): 21-27.

Xu, C.Y. and Singh, V.P. "Evaluation of three complementary relationship evapotranspiration models by water balance approach to estimate actual regional evapotranspiration in different climatic regions." *Journal of Hydrology* 308.1-4 (2005): 105-121.

Zreda, M., Desilets, D., Ferré, T.P.A. and Scott, R.L. "Measuring soil moisture content non-invasively at intermediate spatial scale using cosmic-ray neutrons." *Geophysical research letters* 35.21 (2008): doi.org/10.1029/2008GL035655

Zreda, M., Shuttleworth, W.J., Zeng, X., Zweck, C., Desilets, D., Franz, T. and Rosolem, R. "CRNS: The cosmic-ray soil moisture observing system." *Hydrology and Earth System Sciences* 16.11 (2012): 4079-4099.